Phase-Shift Analysis of Pion-Nucleon Elastic Scattering below 1.6 GeV

P. Bareyre, C. Bricman,* and G. Villet

Département de Physique des Particules Elémentaires, Centre d'Etudes Nucléaires de Saclay, Saclay, France

(Received 14 August 1967)

A phase-shift analysis of π-nucleon elastic scattering has been developed, one energy at a time, up to 1.6-GeV pion kinetic energy. This analysis differs from a previous one in that final experimental data and new polarization measurements are included. Particular care has been taken to have a coherent set of data (2170 experimental points). In addition to the known important effects, the phase shifts of the solution have oscillations coming from the experimental data. It is not possible to say whether the oscillations are due to experimental biases or to physical effects. This analysis is consistent with the one presented by Lovelace at the Thirteenth Berkeley Conference.

I. INTRODUCTION

PHASE-SHIFT analyses have gained increasing interest in the last few years. The reason for this popularity is probably that they have been able to detect the presence of new resonances, most of which show up very little in the total cross section from production experiments or in a plot of the invariant mass from formation experiments.

The formalism of the expansion of the π-nucleon scattering amplitude in a limited number of partial waves is well known (see Appendix). In Cence's[1] and in our previous[2] phase-shift analysis, the only assumption was a regular behavior with energy of the partial waves. Some theoretical considerations are included in the other phase-shift analyses. In the so-called energy-dependent analyses, the variation of the amplitudes or phases of the various partial waves with energy has an *a priori* form which is deduced from the model used. This form is very simple in the work of Roper *et al.*[3]: Breit-Wigner resonant amplitudes and polynomial variation for the phases of the background. More elaborate models based on dispersion relations are used either as starting point in Ref. 4 or as a guide for the parametrization in Ref. 5. The energy-independent analysis by Lovelace[6] makes extensive use of the theory. The starting point of the analysis is the partial-wave dispersion relation calculations[7] for the small waves; those relations are also used to check the final result and to impose a smooth varia-

tion of the amplitudes with energy. This analysis may be considered as the most important work combining theory and fits to the experimental data.

The general belief has been for a long time that the experimental data are not sufficient by themselves for a phase-shift analysis and that theory or hypotheses are also necessary. This fact is probably due to the difficulties encountered in performing nucleon-nucleon analyses.[8] Also, the ambiguities resulting from the analysis of pion-nucleon scattering at 310 MeV[9] had given a general feeling that higher energies analyses were rather hopeless. This analogy with nucleon-nucleon scattering is not valid because the π-N scattering matrix has a much simpler structure. Moreover, the experiments with π mesons are now done with a better accuracy and more systematically than those which were previously available for energies lower than 300 MeV.

In his analysis, Cence[1] has shown that the experimental data he used did not require the presence of phase shifts passing through 90°. However, this analysis does not fit the new and more accurate polarization experiments data and is in disagreement with the dispersion relations predictions for the B amplitude.[10]

In our previous paper,[2] many of the more essential data used were only preliminary. The polarizations and charge-exchange angular distributions are the most important ones to resolve ambiguities; they are published now in their final form. Also new polarization results from Berkeley[11] are available and have been included. We thought it was worthwhile to reconsider our first solution. Although we were more certain of the experimental results, we checked their consistency and in some cases made a selection. We analyzed more carefully the small effects on the partial amplitudes to see if they were really unavoidable. This considerable amount of data has allowed us to extend our analysis up to 1.6 GeV.

* Chercheur agréé IISN Bruxelles. Present address: CERN, Geneva, Switzerland.
[1] J. Cence, Phys. Letters 20, 306 (1966).
[2] P. Bareyre, C. Bricman, A. V. Stirling, and G. Villet, Phys. Letters 18, 342 (1965).
[3] L. D. Roper, Phys. Rev. Letters 12, 342 (1964); L. D. Roper and R. M. Wright, Phys. Rev. 138, B921 (1965); L. D. Roper, R. M. Wright, and B. T. Feld, *ibid.* B190 (1965).
[4] M. Hull and F. Lin, Phys. Rev. 139, B630 (1965).
[5] B. H. Brandsen, P. J. O'Donnell, and R. G. Moorhouse, Phys. Letters 11, 339 (1964); 19, 420 (1965); Phys. Rev. 139, B1566 (1965).
[6] P. Auvil, A. Donnachie, A. T. Lea, and C. Lovelace, Phys. Letters 12, 76 (1964); A. Donnachie, R. G. Kirsopp, A. T. Lea, and C. Lovelace, in *Proceedings of the Thirteenth Annual International Conference on High-Energy Physics, Berkeley, 1966* (University of California Press, Berkeley, 1967).
[7] A. Donnachie, J. Hamilton, and A. T. Lea, Phys. Rev. 135, B515 (1964); J. Hamilton, *Strong Interactions and High Energy Physics*, edited by R. G. Moorhouse (Oliver and Boyd, London, 1964), pp. 281–370.

[8] P. Cziffra, M. H. MacGregor, M. J. Moravcsik, and H. P. Stapp, Phys. Rev. 114, 880 (1959).
[9] O. T. Vik and H. R. Rugge, Phys. Rev. 129, 2311 (1963).
[10] R. Hüper, Z. Physik 181, 426 (1964); K. D. Draxler and R. Hüper, Phys. Letters 20, 199 (1966).
[11] O. Chamberlain, M. J. Hansroul, C. H. Johnson, P. D. Grannis, L. E. Holloway, L. Valentin, P. R. Robrish, and H. M. Steiner, Phys. Rev. Letters 17, 975 (1966); and (private communication); M. J. Hansroul, thesis, University of California Radiation Laboratory Report No. UCRL-17263 (unpublished).
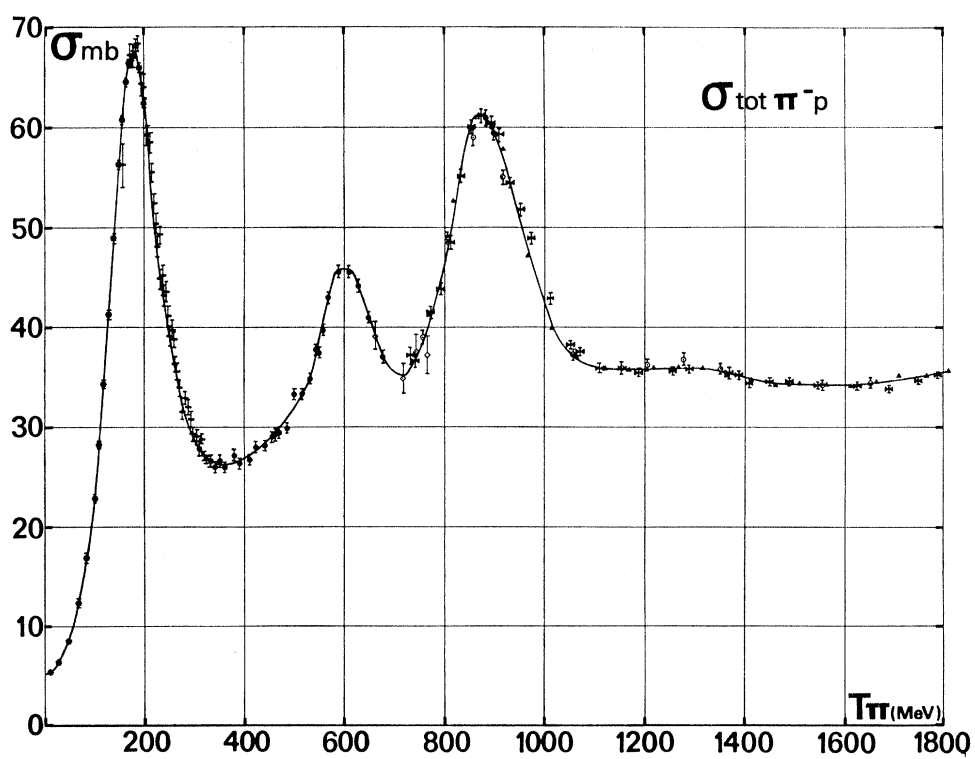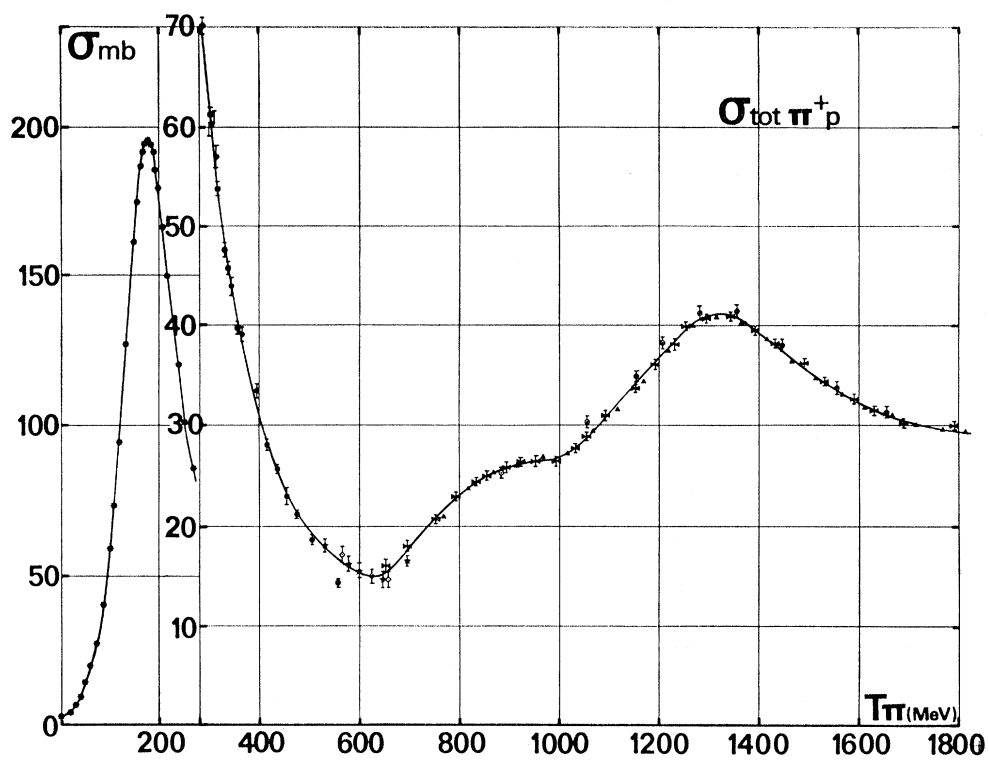
FIG. 1. Total cross section in $\pi^{\pm}p$. The selection of data is discussed in Ref. 42. The curve drawn results from a smoothing done by hand

The method used is not different from that used in Ref. 2 (see Sec. III). A phase-shift analysis is done at all energies where a sufficient number of experimental data are available. Each energy is treated separately and no hypothesis is made for the variation of the partial-wave amplitudes with energy. A rather large number of series of phase shifts is obtained at each energy, and the "best" one is extracted by continuity. This is clearly possible because the energies where the analysis is done are not separated by more than 50 MeV below 1 GeV.

The resulting solution has, in our view, a high probability of being the real solution because, at each energy, the fit of the experimental data is good, and a fair continuity for the variation of the partial-wave amplitudes with energy is assured. It must be pointed out, however, that our method does not permit the detection of the biases in the measurements which is supposed to be the biggest advantage of energy-dependent fits. Thus we cannot assert that our solution is free of spurious oscillations: it is readily seen that, for instance, the coefficients of the expansion of angular distributions in Legendre polynomials do not have an absolutely smooth energy variation.

II. EXPERIMENTAL DATA

A large number of experiments have been done in this energy range on the interaction of π mesons with nucleons.

The experimental data[11-41] available before January

1967 are analyzed and discussed more completely in an internal report.[42] A few comments are made hereafter on these data.

For the total cross sections we used mainly the measurements from Saclay[36] between 300 and 700 MeV and those from Saclay[37] and Brookhaven[38] for higher energies. The measurements from Princeton[39] are in good agreement with the former in the high-energy region and have also been used. The low-energy part is affected by very large systematic errors and has not been considered. The older measurements have been disregarded.[40] As there are a large number of experimental points, the actual value fed in the program was obtained after a smoothing of all the data, the mean accuracy being about 1.5% (Fig. 1).

The total inelastic cross sections are obtained by a more indirect way. The data come mainly from bubble-chamber experiments with the exception of those concerning the neutral channels given by one counter[41] and two spark-chamber experiments.[26,28] The references of the available data except for the very latest ones can be

[12] J. H. Foote, O. Chamberlain, E. H. Rogers, H. M. Steiner, C. E. Wiegand, and T. Ypsilantis, Phys. Rev. 122, 948 (1961).

[13] H. R. Rugge and O. T. Vik, Phys. Rev. 129, 2300 (1963).

[14] J. F. Arens (private communication).

[15] D. L. Lind, B. C. Barish, R. J. Kurz, P. M. Ogden, and V. Perez-Mendez, Phys. Rev. 138, B1509 (1965).

[16] R. E. Hill, N. E. Booth, R. J. Esterling, D. L. Jenkins, N. H. Lipman, H. R. Rugge, and O. T. Vik, Bull. Am. Phys. Soc. 9, 410 (1964).

[17] J. H. Foote, O. Chamberlain, E. H. Rogers, and H. M. Steiner, Phys. Rev. 122, 959 (1961).

[18] P. M. Ogden, D. E. Hagge, J. A. Helland, M. Banner, J. F. Detoeuf, and J. Teiger, Phys. Rev. 137, B1115 (1965).

[19] D. F. Dickinson, J. A. Helland, and V. Perez-Mendez, Phys. Letters 20, 549 (1966).

[20] M. Banner, J. F. Detoeuf, M. L. Fayoux, J. L. Hamel, J. Movchet, L. van Rossum, J. Cheze, J. Teiger, and J. Zsembery, Nuovo Cimento 50A, 431 (1967).

[21] P. Bareyre, C. Bricman, M. J. Longo, G. Valladas, G. Villet, G. Bizard, J. Duchon, J. M. Fontaine, J. P. Patry, J. Seguinot, and J. Yonnet, Phys. Rev. Letters 14, 198 (1965).

[22] P. Bareyre, C. Bricman, M. J. Longo, G. Valladas, G. Villet, G. Bizard, J. Duchon, J. M. Fontaine, J. P. Patry, J. Seguinot, and J. Yonnet, Phys. Rev. Letters 14, 878 (1965).

[23] C. B. Chiu, thesis, University of California Radiation Laboratory Report No. UCRL-6209 (unpublished); C. B. Chiu, R. D. Eandi, A. C. Helmholz, R. W. Kenney, B. J. Moyer, J. A. Poirier, W. B. Richards, R. J. Cence, V. Z. Peterson, N. K. Sehgal, and V. J. Stenger, Phys. Rev. 156, 1415 (1967).

[24] J. A. Helland, C. D. Wood, T. J. Devlin, D. E. Hagge, M. J. Longo, and B. J. Moyer, Phys. Rev. 134, 1062 (1964).

[25] R. D. Eandi, T. J. Devlin, R. W. Kenney, P. G. McManigal, and B. J. Moyer, Phys. Rev. 136, B536 (1964).

[26] J. A. Helland, C. D. Wood, T. J. Devlin, D. E. Hagge, M. J. Longo, B. J. Moyer, and V. Perez-Mendez, Phys. Rev. 134, B1079 (1964).

[27] I. M. Vasilevsky, V. V. Vishnyakov, I. M. Ivachenko, L. I.

Lapidus, I. N. Silin, A. A. Tyapkin, and V. A. Schegelsky, Phys Letters 23, 174 (1966).

[28] F. Bulos, R. E. Lanou, A. E. Pifer, A. M. Shapiro, M. Widgoff, R. Panvini, A. E. Brenner, C. A. Bordner, M. E. Law, E. E. Ronat, K. Strauch, J. Szymanski, P. Bastien, B. B. Brabson, Y. Eisenberg, B. T. Feld, V. K. Fischer, I. A. Pless, L. Rosenson, R. K. Yamamoto, G. Calvelli, L. Guerriero, G. A. Salandin, A. Tomasin, L. Ventura, C. Voci, and F. Waldner, Phys. Rev. Letters 13, 558 (1964).

[29] P. J. Duke, P. J. Jones, M. A. R. Kemp, P. G. Murphy, J. D. Prentice, and J. J. Thresher, Phys. Rev. 149, 1077 (1966).

[30] P. J. Duke, D. P. Jones, M. A. R. Kemp, P. G. Murphy, J. J. Thresher, C. R. Cox, K. S. Head, J. D. Prentice, and R. Atkinson, Rutherford High Energy Laboratory Report No. RPP/H/8 (unpublished).

[31] L. Bertanza, A. Bigi, R. Carrara, and R. Casali, Nuovo Cimento 44A, 712 (1966).

[32] R. D. Eandi, T. J. Devlin, R. W. Kenney, P. G. McManigal, and B. J. Moyer, Phys. Rev. 136, B1187 (1964).

[33] W. Busza, D. G. Davis, B. G. Duff, R. E. Jennings, F. F. Heymann, D. T. Walton, E. H. Bellamy, T. F. Buckley, P. V. March, A. Stafanini, and J. A. Strong, Nuovo Cimento 42A, 871 (1966).

[34] S. Suwa, A. Yokosawa, N. Booth, R. Esterling, and R. Hill, Phys. Rev. Letters 15, 560 (1965).

[35] A. S. Carroll, A. B. Clegg, I. F. Corbett, C. S. J. Damerell, N. Midlemas, D. Newton, T. W. Quirk, and W. S. C. Williams, Proc. Roy. Soc. (London) 289A, 513 (1966).

[36] G. Bizard, J. Duchon, J. Seguinot, J. Yonnet, P. Bareyre, C. Bricman, G. Valladas, and G. Villet, Nuovo Cimento 44A, 999 (1966).

[37] A. V. Stirling, thesis, Commissariat á l'Energie Atomique Report CEA-R 2838 (unpublished).

[38] J. Teiger (private communication); R. L. Cool, G. Giacomelli, T. F. Kycia, B. A. Leontic, K. K. Li, A. Lundby, J. Teiger, and C. Wilkin (to be published).

[39] T. J. Devlin, J. Solomon, and G. Bertsch, Phys. Rev. Letters 14, 1031 (1965).

[40] T. J. Devlin, B. J. Moyer, and V. Perez-Mendez, Phys. Rev. 125, 690 (1962); J. C. Brisson, J. F. Detoeuf, P. Falk-Vairant, L. van Rossum, and G. Valladas, Nuovo Cimento 19, 210 (1961).

[41] J. C. Brisson, P. Falk-Vairant, J. P. Merlo, P. Sonderegger, R. Turlay, and G. Valladas, in Proceedings of the Aix-en-Provence International Conference on Elementary Particles, 1961, edited by E. Cremieu-Alcan et al. (Centre d'Etudes Nucleaires de Saclay, Seine et Oise, 1961), Vol. I, p. 45.

[42] P. Bareyre, C. Bricman, and G. Villet, Commissariat á l'Energie Atomique Report CEA-R 3401 (unpublished).
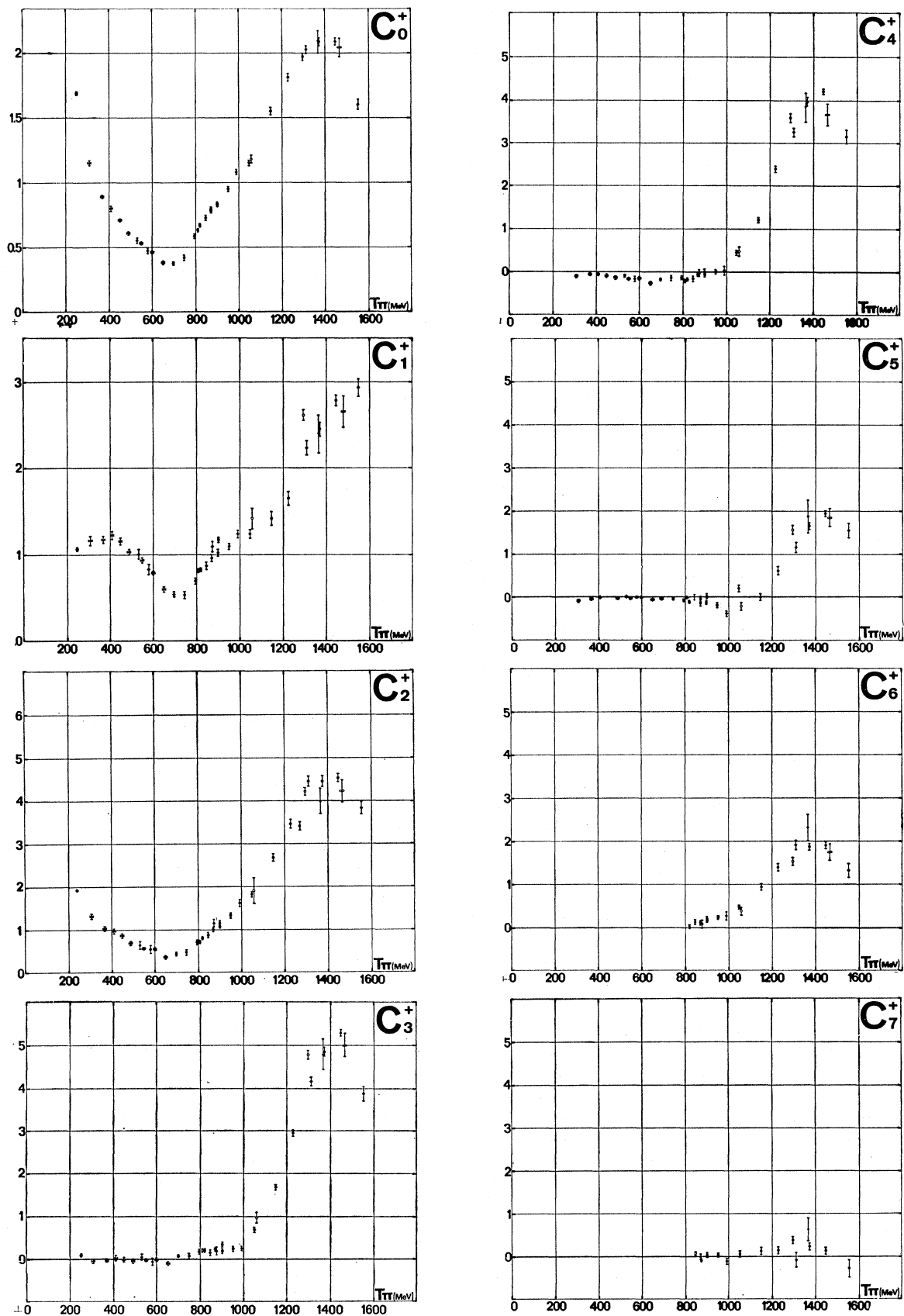
FIG. 2. Coefficients of the expansion of the elastic $\pi^+ p$ angular distributions in Legendre polynomials; see Ref. 42 for references.

found in an earlier paper[43] and in Ref. 36. Here also a smoothing has been done, but the points are much more separated in energy and the errors are larger than those of the total cross section.

The elastic differential cross sections of charged π mesons are rather well known. There are mainly three series of counter measurements Refs. 18 and 24, Refs. 26 and 29, and some hydrogen bubble-chamber results with good statistics (see footnotes in Ref. 42). The usual way of summarizing those results is to give the coefficients C_n of the expansion of those distributions in Legendre polynomials:

$$d\sigma/d\Omega = \lambda^2 \sum_n C_n P_n(\cos\theta). \quad \text{[Eq. (A9) in Appendix]}$$

To give an idea of the consistency of the measurements, Figs. 2 and 3 show the coefficients $C_n^\pm$ obtained by a method described in Ref. 42, which includes the usual precautions regarding the order of the expansion. However, it must be pointed out that sometimes, when two measurements of comparable accuracy exist for the same energy, the agreement is not always good. In those cases, the final choice was made on the basis of which measurement gave the "better" solution, i.e., the one with the lower χ^2, or if both solutions have almost the same χ^2, the one for which the continuity was easier to achieve. Stated in other terms, the chosen distribution allows a smoother variation of the coefficients C_n. This choice is not above all criticism, but seems to be the most reasonable one. To enter both distributions would have the same result as entering the average of the two distributions, the χ^2 being certainly very bad; this is not easier to justify.

As the C_n coefficients have been obtained at energy intervals generally smaller than 50 MeV, it is possible to predict with a linear interpolation the angular distributions for any energy below 1.6 GeV. This interpolation has been applied to obtain with a rather good degree of confidence the angular distribution in a few cases, where there is no measurement available.

The charge-exchange differential cross sections have been measured at many energies with heavy-plate spark chambers.[28,23] The charge-exchange coefficients C_n^0 of the expansion in Legendre polynomials have larger statistical and systematic errors than in the charged final states. However, their variation with energy is well defined (Fig. 4). These coefficients have been used to obtain the angular distributions by linear interpolation at the energies where they are missing (i.e., for 775, 795, 845, 950, 1048, and 1227 MeV). As large errors have been attached to these interpolated coefficients, this procedure cannot introduce any bias in the analysis.

Only one point at 310 MeV exists for the polarization of the neutron in $\pi^- p \rightarrow \pi^0 n$. The polarization of the proton in elastic scattering has been measured by many groups. With the exception of the 410- and 490-MeV

experiments, Refs. 21 and 22, the results obtained by using a polarized proton target at Nimrod,[30] Berkeley,[14] and Argonne[34] are much more accurate than the first results where the polarization of the proton was analyzed by a second scattering on carbon. It seems that the polarization measurements are of great importance to reduce the hugh number of phase-shift series which can fit the differential cross sections. Unfortunately, they were not always done at energies where measurements of differential cross sections already existed; this fact somewhat reduces the interest of such measurements. They were used together with constructed angular distributions using the interpolated values of the coefficients C_n as explained above. The phase shifts obtained with these distributions are however certainly less reliable than those found for energies where all the data are available. It should be noted that it is not possible to "construct" polarization data by the method used for the differential cross sections. Only for some measurements is the expansion of

$$P(d\sigma/d\Omega)/\sin\theta = \lambda^2 \sum_n D_n P_n(\cos\theta)$$
$$\text{[Eq. (A12) in Appendix]}$$

meaningful; for the others, either the accuracy is too low, or the polarization is known in a too restricted angular range to allow the determination of more than 2 or 3 coefficients. The maximum order of those expansions does not show the presence of F or G waves even when they are required by the angular distributions (Figs. 5 and 6).

III. METHOD AND RESULTS

The first step of our analysis is to perform single-energy fits; this is done with a fairly simple program. Starting from any set of phase shifts, the program computes the theoretical values of the given experimental data. The usual formulas, which can be found in many textbooks, have been used; they are summarized in the Appendix. The Coulomb corrections are those given in Ref. 3. The total number of $\pi^\pm p$ scattering data points was equal to 2170. It included the total cross sections and total inelastic cross sections at all energies and, when measured, the elastic and charge-exchange differential cross-section points and the recoil nucleon polarization points (see Sec. II for the special cases where the differential cross sections were missing). The forward cross sections obtained from dispersion relations were also used.[44]

The resulting χ^2 is deduced by the sum

$$\chi^2 = \sum_i \left(\frac{G_{ie} - G_{ic}}{\Delta G_i}\right)^2,$$

where G_c is the computed value, and G_e and ΔG the value and the error of the fitted quantity. The phases and

[43] P. Bareyre, C. Bricman, G. Valladas, G. Villet, J. Bizard, and J. Seguinot, Phys. Letters 8, 137 (1964).

[44] G. Höhler, G. Ebel, and G. S. Giesecke, Z. Physik 180, 430 (1964); and (private communication).
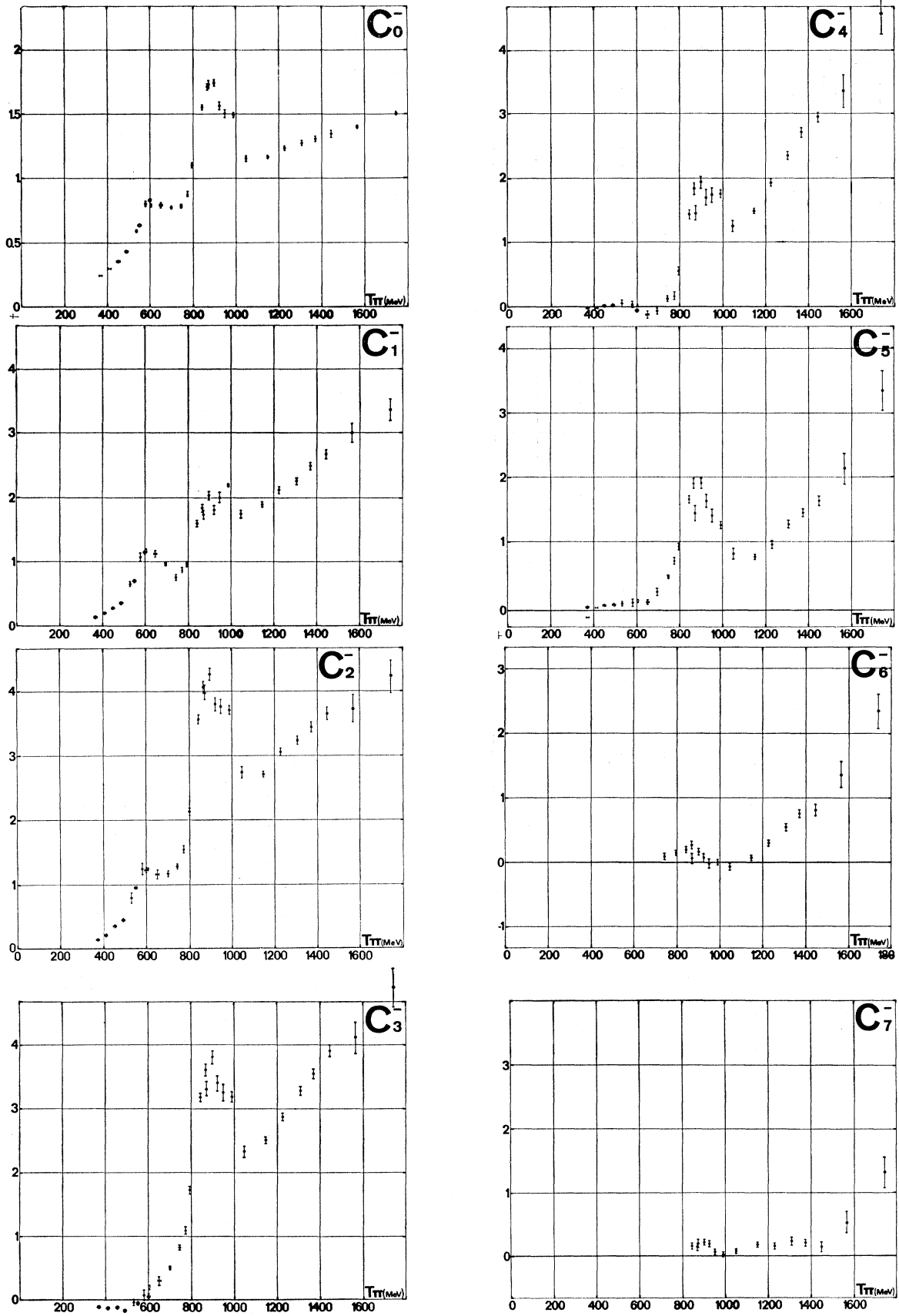
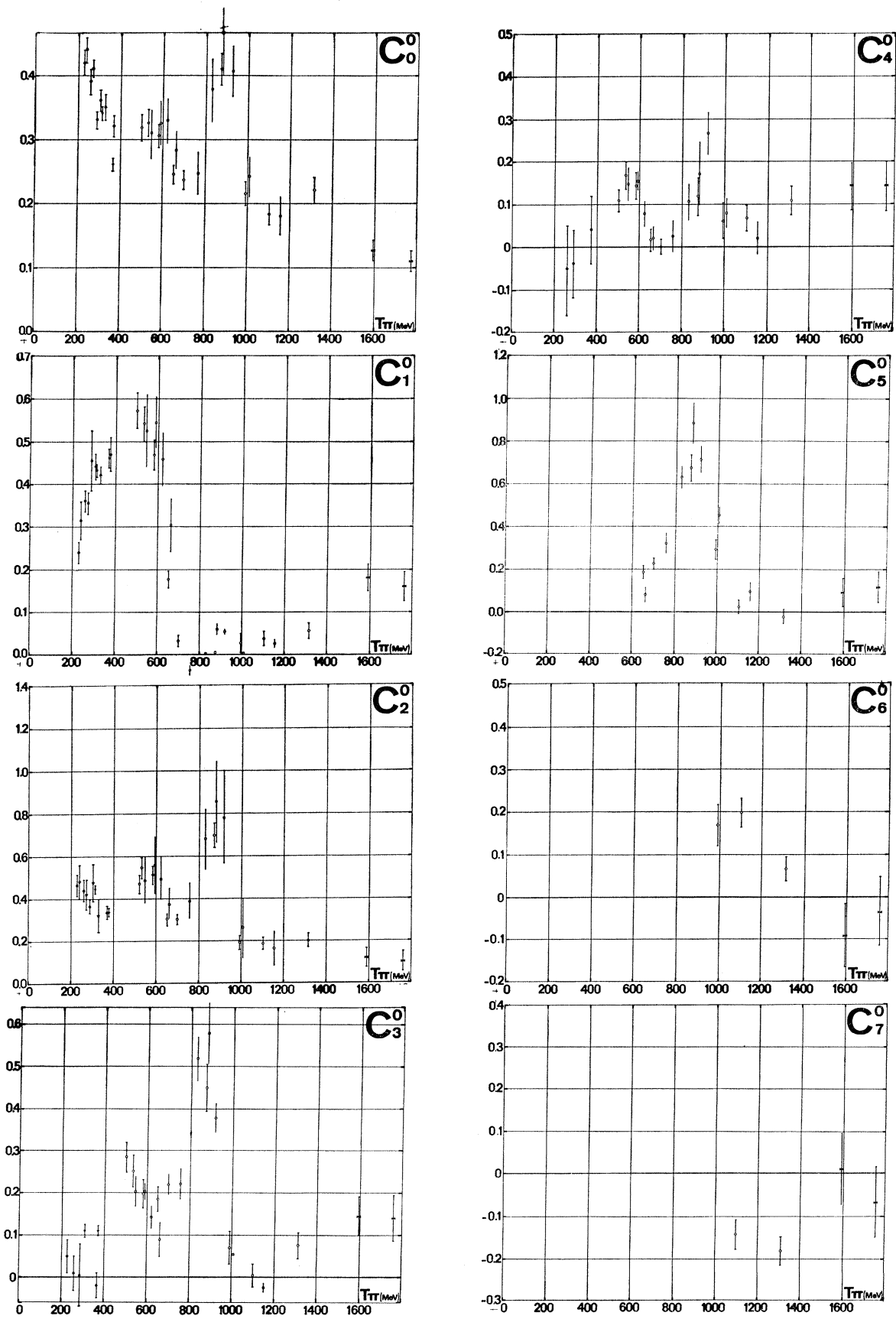FIG. 3. Same as Fig. 2 for π^-p scattering.

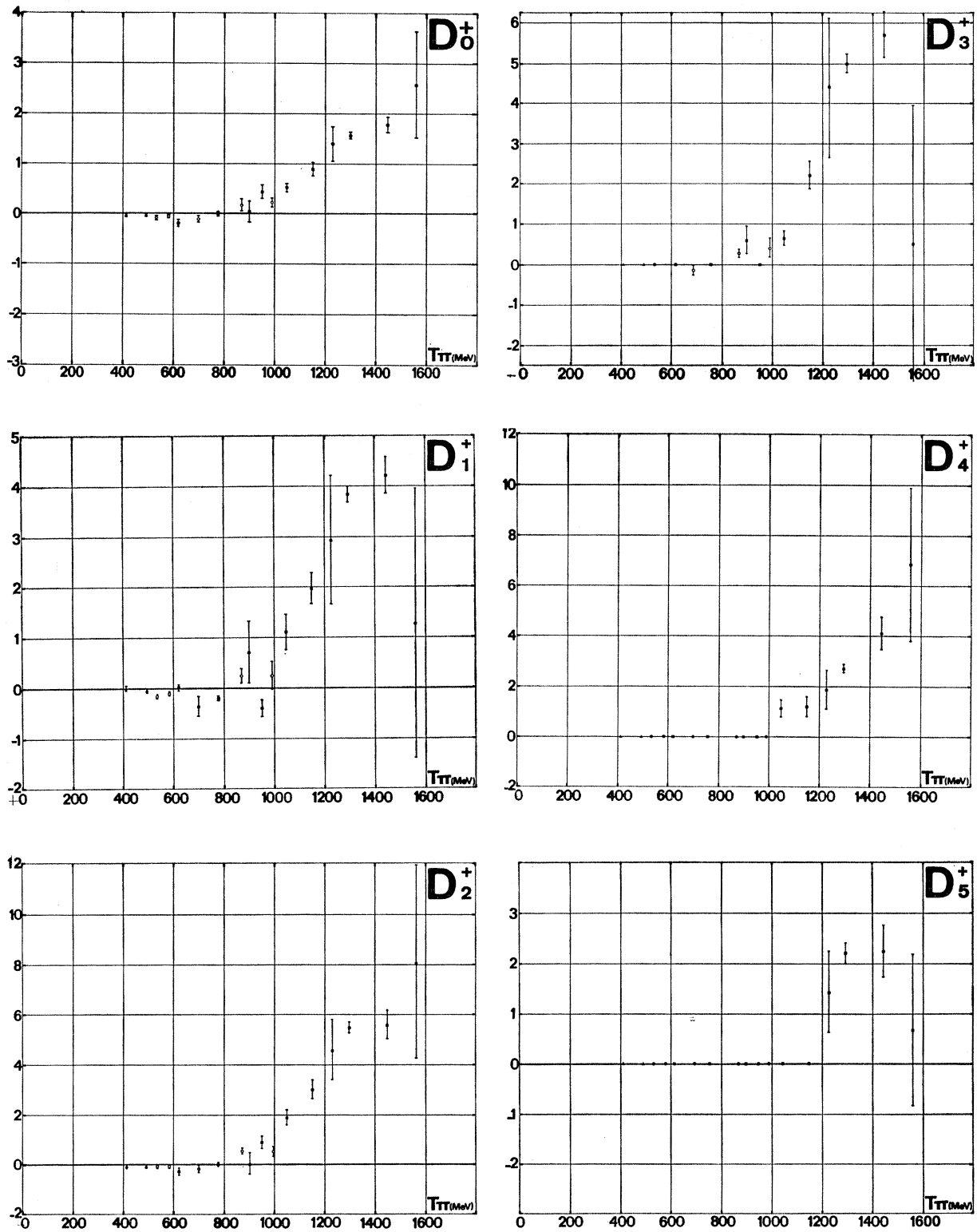FIG. 4. Same as Fig. 2 for charge-exchange scattering.

FIG. 5. $D_n{}^+$ coefficients of the expansion of $1/(\lambda^2 \sin\theta)P(d\sigma/d\Omega)$ in Legendre polynomials for π^+p elastic scattering.
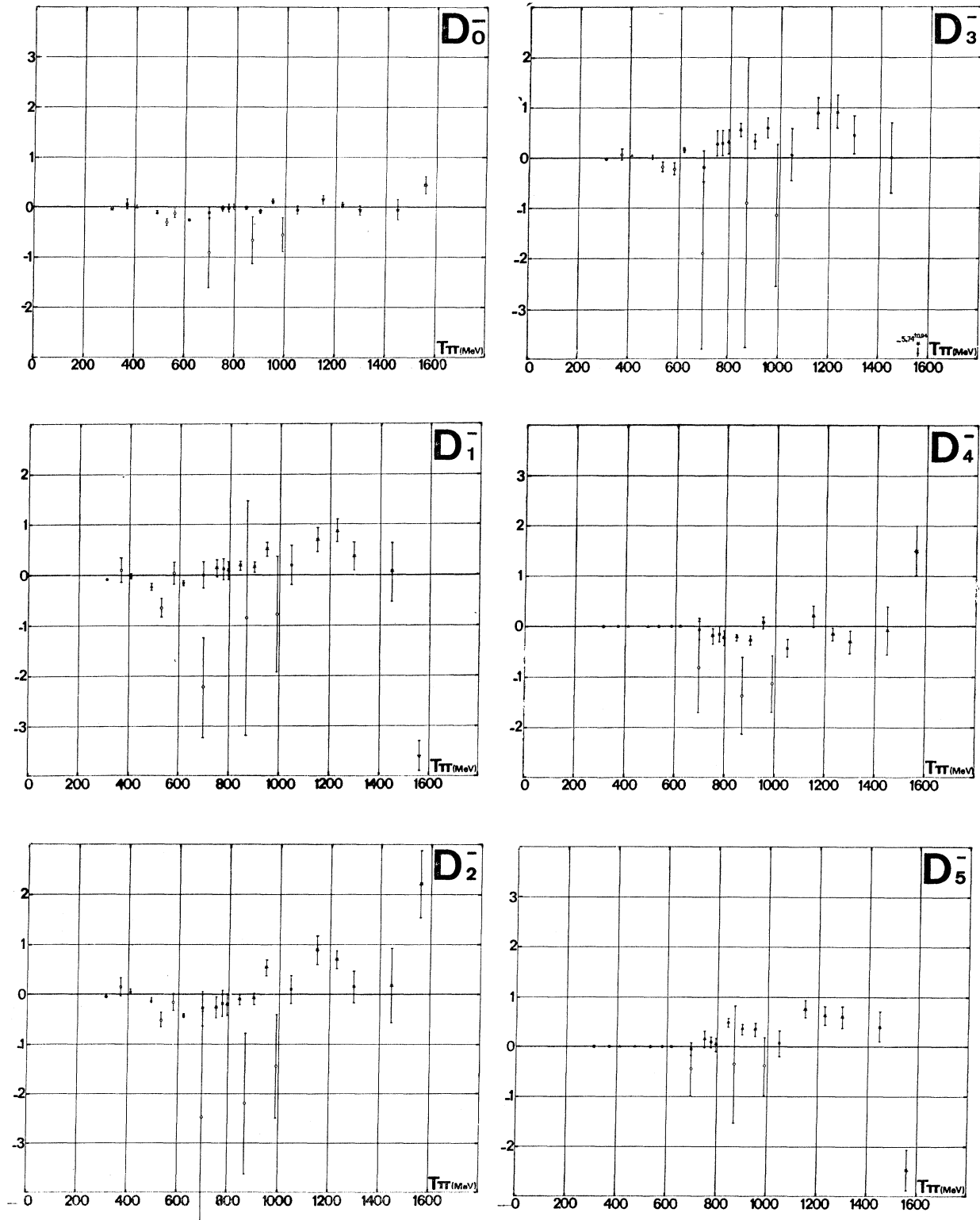
FIG. 6. Same as Fig. 5 for $\pi^- p$ scattering.

TABLE I. Value of the phase shifts δ (deg) and absorption parameters ρ for the final solution A in the $I = \frac{3}{2}$ state.

T_π (MeV)		S_{31}	P_{31}	P_{33}	D_{33}	D_{35}	F_{35}	F_{37}	G_{37}	G_{39}
310	δ	$-20.4\ \pm0.3$	$-9.5\ \pm0.3$	$-42.9\ \pm0.2$	$-1.7\ \pm0.3$	$-0.5\ \pm\ 0.2$	$-0.9\ \pm0.2$	$2.0\ \pm0.3$		
	ρ	1.0	1.0	1.0	1.0	1.0	1.0	1.0		
370	δ	$-25.8\ \pm0.6$	$-8.5\ \pm0.5$	-35.5 ± 0.3	$0.0\ \pm0.3$	$-1.0\ \pm\ 0.4$	$1.1\ \pm0.3$	$-0.7\ \pm0.9$		
	ρ	1.0	1.0	1.0	1.0	1.0	0.99 ± 0.01	1.0		
410	δ	$-24.0\ \pm0.3$	$-11.6\ \pm0.6$	$-31.3\ \pm0.3$	$0.2\ \pm0.3$	$-1.9\ \pm\ 0.3$	$-1.3\ \pm0.2$	$2.3\ \pm0.2$		
	ρ	0.99 ± 0.01	0.96 ± 0.01	1.0	1.0	1.0	0.99 ± 0.01	1.0		
492	δ	$-24.7\ \pm0.6$	$-10.6\ \pm1.2$	$-24.6\ \pm0.5$	$4.3\ \pm0.5$	$-5.3\ \pm\ 0.7$	$0.7\ \pm0.4$	$0.2\ \pm0.4$		
	ρ	0.87 ± 0.01	0.99 ± 0.01	1.0	1.0	1.0	1.0	1.0		
533	δ	$-28.4\ \pm0.9$	$-11.4\ \pm1.7$	$-21.5\ \pm0.8$	$2.4\ \pm0.7$	$-4.7\ \pm\ 0.8$	$-0.5\ \pm0.6$	$1.5\ \pm0.6$		
	ρ	0.92 ± 0.02	0.89 ± 0.04	0.99 ± 0.01	0.98 ± 0.02	1.0	1.0	1.0		
581	δ	$-27.6\ \pm1.1$	$-13.3\ \pm3.2$	$-18.3\ \pm1.1$	$3.7\ \pm1.9$	$-4.5\ \pm\ 4.0$	$0.7\ \pm0.7$	$1.4\ \pm0.6$		
	ρ	0.89 ± 0.05	0.90 ± 0.06	0.95 ± 0.03	$0.99_{-0.03}^{+0.01}$	1.0	1.0	1.0		
618	δ	$-26.9\ \pm1.1$	$-20.5\ \pm2.0$	$-13.1\ \pm1.0$	$-1.0\ \pm1.0$	$-0.6\ \pm\ 0.8$	$-0.9\ \pm0.7$	$3.4\ \pm0.7$		
	ρ	0.96 ± 0.04	1.0	1.0	0.90 ± 0.04	1.0	0.94 ± 0.02	1.0		
650	δ	$-25.1\ \pm1.7$	$-18.8\ \pm1.1$	$-10.2\ \pm1.0$	$1.7\ \pm1.6$	$-2.6\ \pm\ 0.9$	$1.0\ \pm0.7$	$3.2\ \pm0.6$		
	ρ	0.91 ± 0.05	0.97 ± 0.03	1.0	0.76 ± 0.04	1.0	0.97 ± 0.03	1.0		
698	δ	$-26.2\ \pm2.0$	$-18.9\ \pm1.3$	$-10.3\ \pm0.8$	$-0.3\ \pm0.9$	$-3.3\ \pm\ 1.2$	$-1.3\ \pm1.0$	$4.8\ \pm0.9$	$-0.5\ \pm0.5$	$0.6\ \pm0.5$
	ρ	0.68 ± 0.08	1.0	0.95 ± 0.02	0.89 ± 0.01	$0.99\pm\ 0.01$	0.99 ± 0.01	1.0	1.0	0.96 ± 0.01
750	δ	$-24.8\ \pm2.6$	$-24.8\ \pm2.1$	$-11.2\ \pm1.2$	$1.4\ \pm2.0$	$-1.5\ \pm\ 0.9$	$0.7\ \pm1.0$	$2.0\ \pm0.6$	$-0.3\ \pm0.6$	$0.7\ \pm0.4$
	ρ	0.56 ± 0.06	$0.99_{-0.05}^{+0.01}$	0.94 ± 0.05	0.94 ± 0.06	$0.90\pm\ 0.03$	0.91 ± 0.04	1.0	1.0	0.98 ± 0.02
775	δ	$-30.7\ \pm1.8$	$-28.7\ \pm1.9$	$-10.8\ \pm1.1$	$3.1\ \pm2.4$	$-1.2\ \pm\ 0.7$	$2.6\ \pm1.1$	$1.8\ \pm0.7$	$-0.1\ \pm0.8$	$0.1\ \pm0.5$
	ρ	0.38 ± 0.04	0.84 ± 0.05	0.93 ± 0.05	0.90 ± 0.03	$0.83\pm\ 0.04$	$0.99_{-0.03}^{+0.01}$	1.0	1.0	1.0
795	δ	$-25.5\ \pm2.1$	$-28.6\ \pm1.7$	$-12.2\ \pm1.1$	$6.0\ \pm3.6$	$-1.7\ \pm\ 0.8$	$5.1\ \pm1.9$	$2.0\ \pm0.7$	$2.0\ \pm0.8$	$0.1\ \pm0.4$
	ρ	0.22 ± 0.04	0.81 ± 0.07	0.85 ± 0.04	0.92 ± 0.04	$0.84\pm\ 0.04$	$0.99_{-0.04}^{+0.01}$	1.0	1.0	1.0
845	δ	$-42.4\ \pm1.4$	$-26.3\ \pm4.1$	$-10.8\ \pm1.3$	$-1.4\ \pm0.5$	$-7.1\ \pm\ 0.5$	$2.1\ \pm1.0$	$7.4\ \pm0.5$	$1.8\ \pm0.4$	$-1.6\ \pm0.4$
	ρ	0.46 ± 0.02	0.93 ± 0.02	0.82 ± 0.02	1.0	$0.84\pm\ 0.02$	0.97 ± 0.02	1.0	1.0	0.93 ± 0.02
873	δ	$-61.7\ \pm0.9$	$-13.2\ \pm1.3$	$-7.3\ \pm0.8$	$-1.6\ \pm1.8$	$-6.3\ \pm\ 0.8$	$1.7\ \pm0.6$	$5.7\ \pm0.4$	$-1.3\ \pm0.5$	$1.6\ \pm0.4$
	ρ	0.65 ± 0.03	0.90 ± 0.03	0.73 ± 0.01	0.97 ± 0.02	$0.76\pm\ 0.01$	0.96 ± 0.02	0.99 ± 0.01	1.0	1.0
900	δ	$-55.1\ \pm1.0$	$-24.2\ \pm0.9$	$-6.5\ \pm0.9$	$-2.2\ \pm0.6$	$-6.8\ \pm\ 0.5$	$2.6\ \pm0.5$	$8.3\ \pm0.4$	$1.0\ \pm0.4$	$0.1\ \pm0.4$
	ρ	0.64 ± 0.02	0.90 ± 0.02	0.77 ± 0.02	0.88 ± 0.02	$0.85\pm\ 0.01$	0.92 ± 0.02	1.0	1.0	0.96 ± 0.01
950	δ	$-66.7\ \pm3.1$	$-14.2\ \pm2.0$	$-3.2\ \pm2.2$	$-8.5\ \pm1.6$	$-2.2\ \pm\ 1.8$	$3.8\ \pm0.7$	$9.0\ \pm0.6$	$-0.3\ \pm0.6$	$1.2\ \pm0.8$
	ρ	0.62 ± 0.03	0.84 ± 0.05	0.66 ± 0.10	0.62 ± 0.03	$0.92\pm\ 0.02$	0.97 ± 0.02	1.0	1.0	1.0
990	δ	$-56.1\ \pm1.4$	$-16.3\ \pm1.1$	$-8.2\ \pm2.6$	$-9.6\ \pm1.3$	$-3.4\ \pm\ 1.5$	$3.3\ \pm0.8$	$11.3\ \pm3.5$	$-3.1\ \pm0.8$	$3.2\ \pm0.8$
	ρ	0.82 ± 0.06	$0.97_{-0.08}^{+0.03}$	0.80 ± 0.07	0.77 ± 0.04	$0.77\pm\ 0.14$	0.87 ± 0.07	0.99 ± 0.01	1.0	1.0
1048	δ	$-50.5\ \pm2.9$	$-26.0\ \pm2.1$	$1.0\ \pm1.9$	$-12.3\ \pm1.3$	$-2.2\ \pm\ 1.5$	$-0.6\ \pm1.0$	$14.9\ \pm0.9$	$-0.3\ \pm0.7$	$-0.3\ \pm0.8$
	ρ	0.83 ± 0.07	$0.97_{-0.05}^{+0.03}$	0.91 ± 0.04	0.90 ± 0.02	$0.84\pm\ 0.03$	0.76 ± 0.02	0.88 ± 0.02	0.91 ± 0.02	1.0
1150	δ	$-65.6\ \pm3.1$	$-18.6\ \pm3.7$	$-1.6\ \pm1.6$	$-16.6\ \pm1.5$	$1.0\ \pm\ 1.9$	$-0.5\ \pm1.5$	$19.7\ \pm0.9$	$-0.4\ \pm0.7$	$-0.8\ \pm0.9$
	ρ	0.83 ± 0.05	0.71 ± 0.10	0.96 ± 0.04	0.89 ± 0.03	$0.70\pm\ 0.05$	0.70 ± 0.02	0.90 ± 0.04	0.98 ± 0.02	0.92 ± 0.03
1227	δ	$-72.2\ \pm4.6$	$-21.6\ \pm3.1$	$1.5\ \pm2.0$	$-14.9\ \pm1.6$	$-3.3\ \pm\ 1.4$	$1.7\ \pm1.0$	$22.6\ \pm2.6$	$-1.7\ \pm1.0$	$0.2\ \pm0.9$
	ρ	0.87 ± 0.09	0.54 ± 0.04	1.0	0.79 ± 0.03	$0.60\pm\ 0.03$	0.74 ± 0.02	0.93 ± 0.04	0.94 ± 0.03	1.0
1300	δ	$-72.6\ \pm3.2$	$-9.5\ \pm4.4$	$1.4\ \pm2.1$	$-12.6\ \pm1.3$	$-6.8\ \pm\ 2.6$	$-0.7\ \pm1.2$	$30.4\ \pm1.5$	$0.8\ \pm0.7$	$-0.6\ \pm1.4$
	ρ	0.59 ± 0.06	0.37 ± 0.06	0.84 ± 0.06	0.86 ± 0.04	$0.47\pm\ 0.03$	0.65 ± 0.04	0.66 ± 0.05	1.0	0.98 ± 0.02
1446	δ	$-48.8\ \pm4.2$	$-18.8\ \pm2.9$	$-10.8\ \pm1.7$	$-7.0\ \pm1.0$	$-11.5\ \pm\ 1.6$	$-4.5\ \pm1.0$	$-60.6\ \pm4.3$	$-1.6\ \pm0.7$	$0.4\ \pm0.8$
	ρ	0.49 ± 0.12	0.69 ± 0.06	0.82 ± 0.05	0.88 ± 0.02	$0.66\pm\ 0.05$	0.87 ± 0.02	0.25 ± 0.04	1.0	0.95 ± 0.03
1560	δ	$-1.5\ \pm4.8$	$-13.1\ \pm5.0$	$-34.0\ \pm3.8$	$-16.1\ \pm2.6$	$-23.6\ \pm11.0$	$5.6\ \pm1.8$	$13.6\ \pm1.3$	$-3.9\ \pm1.0$	$0.3\ \pm1.0$
	ρ	0.60 ± 0.12	0.68 ± 0.06	0.63 ± 0.12	0.63 ± 0.08	$0.38\pm\ 0.14$	0.67 ± 0.06	0.65 ± 0.08	1.0	1.0

absorption parameters are then varied to minimize the χ^2 using the steepest-descent method. The time needed to get a solution is rather variable, depending on the number of experimental data used and on the difference between the final and starting values (i.e., the number of iterations), a typical time being 1 to 2 min per good solution, for an IBM 7094 computer. For each energy, the first stage of the search is to get a large number of solutions starting from random sets of parameters. To spare computer time, the starting point for the parameters of the small waves was chosen in a limited range, using the knowledge of the range of variation of that parameter for the preceding energies. This range was never smaller than 50° and 0.5 for phase shift and absorption parameters, respectively. In any case, a solution falling out of this range would have been rejected as noncontinuous at the next stage of the analysis.

The search was done using S, P, D, and F waves up to 698 MeV; for higher energies, we also included G waves, although they are not needed before 900 MeV according to the usual criteria of statistics. In fact, between 700 and 900 MeV all good solutions ended with G waves smaller than 3°. On the average, about 200 starting points were tried at each energy. A small proportion of them gave no useful result, as the χ^2 remained very high, the program finding no way out of a false minimum. The others converged towards a not-too-large number of solutions. For most of the energies, there is a separation between two groups of solutions, the first having a χ^2 smaller than about 1.3 times the best χ^2 found for the same energy ($\chi_{\min}^2$), the other containing solutions with a much higher χ^2. In those cases, only the first group of solutions is retained for the second stage of the analysis. When the χ^2 of the solutions form an almost continuous spectrum, we only keep the solutions for which $\chi^2 < 1.5\chi_{\min}^2$. After this selection, the number
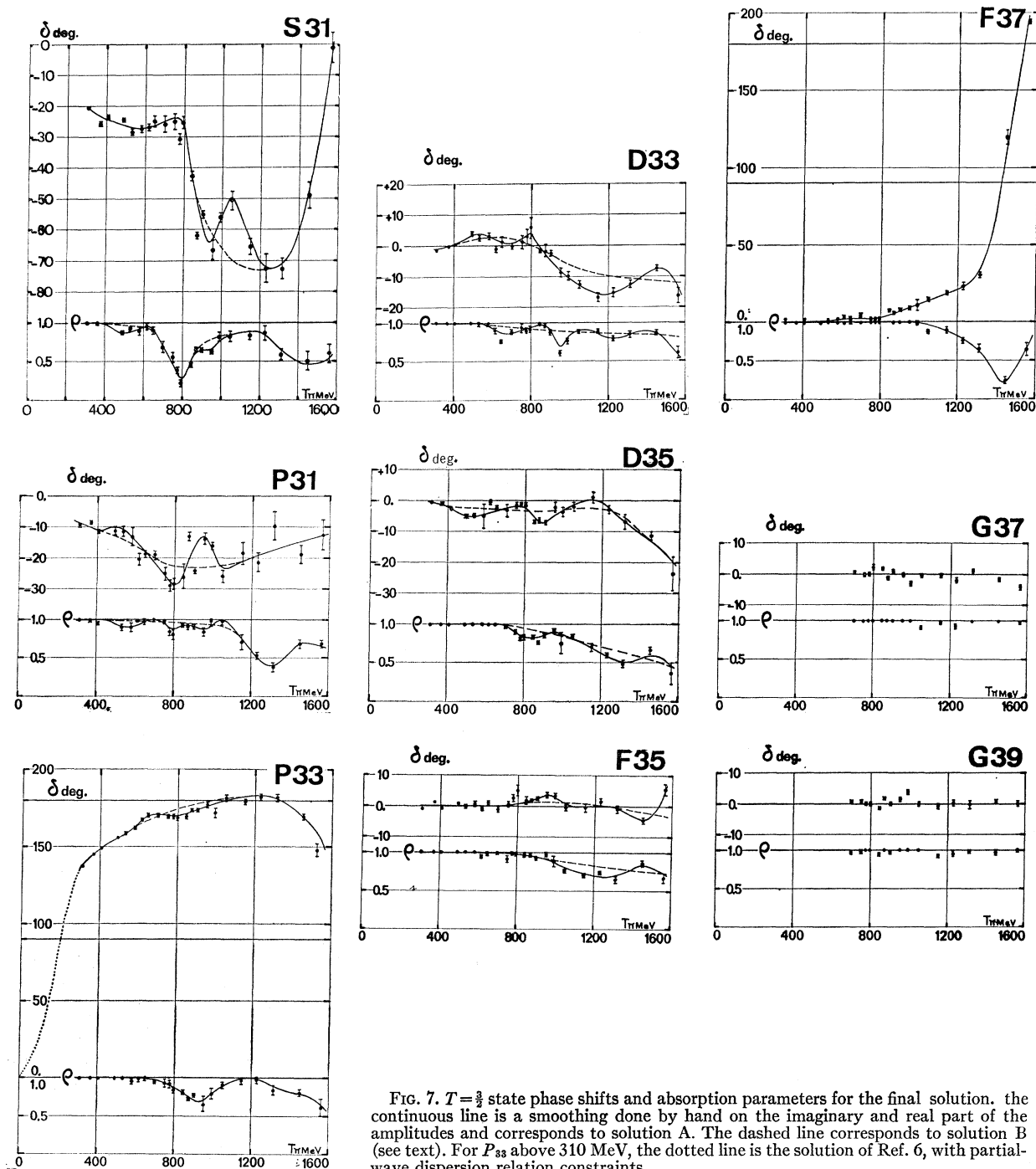
FIG. 7. $T=\frac{3}{2}$ state phase shifts and absorption parameters for the final solution. the continuous line is a smoothing done by hand on the imaginary and real part of the amplitudes and corresponds to solution A. The dashed line corresponds to solution B (see text). For P_{33} above 310 MeV, the dotted line is the solution of Ref. 6, with partial-wave dispersion relation constraints.

of remaining solutions is always smaller than 15, including some scarcely different solutions.

The problem is now the selection of the best solution among the many possible ones at each energy. The spacing between the energies where an analysis has been done corresponds to an interval of about 25-MeV total energy. In such a small interval, one does not expect to observe dramatic variations of the partial-wave parameters. We have required that no anomaly should have occurred in the variation with energy of the following quantities:

(a) The phase δ and the inelasticity parameter ρ for each wave.

TABLE II. Value of the phase shifts δ (deg) and absorption parameters ρ for the final solution A in the $I = \frac{1}{2}$ state.

T_π (MeV)		S_{11}	P_{11}	P_{13}	D_{13}	D_{15}	F_{15}	F_{17}	G_{17}	G_{19}
310	δ	12.3 ± 0.3	22.2 ± 0.3	−3.8 ±0.5	5.7 ±0.2	1.0 ±0.3	1.4 ±0.2	−0.9 ±0.3		
	ρ	1.0	0.99± 0.01	0.96±0.01	0.99±0.01	1.0	1.0	1.0		
370	δ	12.3 ± 0.8	26.5 ± 0.7	−7.8 ±0.2	5.7 ±0.3	0.8 ±0.2	1.2 ±0.2	−2.3 ±0.2		
	ρ	0.96± 0.02	0.96± 0.02	0.98±0.02	1.	1.	0.99±0.01	0.98±0.01		
410	δ	12.1 ± 0.8	34.3 ± 0.4	−7.6 ±0.4	9.7 ±0.3	3.1 ±0.3	2.8 ±0.2	−2.1 ±0.3		
	ρ	1.0	0.88± 0.01	0.91±0.01	0.96±0.01	1.0	1.0	0.99±0.01		
492	δ	26.7 ± 0.8	45.4 ± 0.6	−9.3 ±0.9	16.7 ±0.8	5.7 ±0.8	2.7 ±0.3	−0.3 ±0.3		
	ρ	0.95± 0.01	0.65± 0.02	1.0	0.83±0.02	1.0	0.98±0.01	0.99±0.01		
533	δ	23.7 ± 2.0	63.9 ± 2.7	−8.2 ±1.1	28.9 ±3.4	4.1 ±1.0	4.1 ±2.3	−0.2 ±0.7		
	ρ	1.0	0.42± 0.05	0.91±0.09	0.89±0.06	0.93±0.02	0.98±0.02	0.99±0.01		
581	δ	30.1 ± 1.9	73.5 ± 5.8	−17.1 ±1.8	38.3 ±1.0	2.9 ±1.2	2.4 ±1.2	0.6 ±0.8		
	ρ	0.66± 0.02	0.40± 0.04	0.79±0.06	0.69±0.08	0.90±0.03	0.99±0.01	1.0		
618	δ	38.9 ± 3.0	−66.1 ± 2.8	−11.1 ±0.8	62.8 ±8.7	6.8 ±0.7	6.8 ±1.1	−0.8 ±0.7		
	ρ	0.44± 0.06	0.53± 0.02	0.80±0.03	0.09±0.07	1.0	1.0	0.99±0.01		
650	δ	37.5 ± 5.7	−48.3 ± 1.9	−7.2 ±0.7	−38.8 ±1.0	9.9 ±0.6	10.7 ±0.6	1.4 ±0.4		
	ρ	0.20± 0.03	0.52± 0.03	0.87±0.02	0.53±0.03	0.88±0.02	0.99±0.01	1.0		
698	δ	25.6 ± 3.5	−51.7 ± 2.7	−13.8 ±0.5	−24.5 ±0.8	16.1 ±0.4	9.6 ±0.5	1.2 ±0.4	2.5 ±0.4	0.0 ±0.3
	ρ	0.18± 0.03	0.43± 0.03	1.0	0.61±0.02	0.92±0.02	0.98±0.01	0.92±0.01	0.96±0.01	1.0
750	δ	29.6 ±10.5	−46.3 ± 4.6	−8.2 ±1.3	−28.9 ±1.6	11.9 ±1.1	19.7 ±1.2	−0.2 ±0.5	−0.4 ±0.7	−0.5 ±0.4
	ρ	0.47± 0.6	0.19± 0.08	0.73±0.06	0.79±0.06	0.78±0.04	1.0	1.0	0.98±0.02	0.99±0.01
775	δ	27.1 ± 2.2	−52.6 ±13.6	−8.1 ±1.6	−29.4 ±2.3	15.2 ±1.1	22.4 ±1.6	−1.4 ±0.7	1.6 ±0.9	0.1 ±0.5
	ρ	0.52± 0.03	0.08± 0.08	0.77±0.04	0.76±0.08	0.81±0.04	0.88±0.04	1.0	0.95±0.03	1.0
795	δ	37.5 ± 1.5	0.0	−10.0 ±1.5	−25.0 ±1.2	23.7 ±2.2	22.9 ±1.2	−0.3 ±0.8	2.3 ±0.8	1.3 ±0.5
	ρ	0.86± 0.06	$0.01_{-0.01}^{+0.03}$	0.74±0.06	0.67±0.05	0.72±0.03	0.94±0.06	0.93±0.02	1.0	0.99±0.01
845	δ	59.7 ± 1.4	−50.6 ± 5.6	−14.4 ±4.1	−27.5 ±0.8	15.2 ±2.0	42.9 ±1.1	−3.9 ±0.6	−0.8 ±0.6	−0.6 ±0.5
	ρ	0.63± 0.10	0.23± 0.04	0.85±0.03	0.97±0.03	0.34±0.03	0.44±0.03	0.99±0.01	0.99±0.01	0.92±0.02
873	δ	78.1 ± 2.1	−24.0 ± 9.3	−15.5 ±1.5	−15.7 ±2.1	2.7 ±7.1	47.1 ±3.8	−3.5 ±1.0	−4.1 ±1.0	2.0 ±0.9
	ρ	0.92± 0.03	0.11± 0.07	0.80±0.03	1.0	0.12±0.02	0.19±0.05	1.0	0.90±0.02	0.97±0.02
900	δ	76.7 ± 1.8	−27.2 ± 2.9	−10.3 ±0.8	−21.5 ±0.8	−3.4 ±2.6	79.3 ±2.2	−2.3 ±0.6	0.9 ±0.5	−1.0 ±0.5
	ρ	0.64± 0.02	0.31± 0.03	0.83±0.02	0.79±0.05	0.20±0.02	0.27±0.01	0.99±0.01	1.0	0.94±0.01
950	δ	−75.2 ± 3.2	13.6 ± 6.9	7.1 ±2.4	−2.5 ±2.4	−15.8 ±2.2	−46.5 ±1.4	1.4 ±0.8	3.6 ±0.8	−0.6 ±0.6
	ρ	0.69± 0.05	0.33± 0.06	0.73±0.03	0.62±0.04	0.43±0.03	0.41±0.03	1.0	0.95±0.02	1.0
990	δ	−70.2 ± 1.8	2.4 ± 3.3	2.1 ±1.3	−14.2 ±1.0	−13.2 ±1.0	−30.1 ±1.5	3.8 ±1.4	0.9 ±0.9	3.9 ±0.7
	ρ	0.76± 0.03	0.38± 0.08	0.67±0.03	0.88±0.08	0.44±0.04	0.60±0.05	0.92±0.02	0.99±0.01	0.94±0.02
1048	δ	−61.4 ± 5.9	9.0 ± 3.8	−4.6 ±2.4	−8.6 ±2.4	−16.7 ±1.1	−20.3 ±1.5	−0.4 ±0.9	4.7 ±0.7	2.4 ±0.7
	ρ	0.75± 0.07	0.37± 0.09	0.48±0.04	0.74±0.05	0.81±0.03	0.72±0.04	0.94±0.02	0.89±0.03	1.0
1150	δ	−63.8 ± 1.6	9.0 ± 4.8	−4.4 ±2.4	−10.7 ±2.6	−14.6 ±1.3	−14.4 ±1.6	−1.9 ±0.9	5.9 ±0.9	2.6 ±0.8
	ρ	0.49± 0.03	0.23± 0.07	0.45±0.05	0.68±0.04	$0.97_{-0.05}^{+0.03}$	0.69±0.03	0.82±0.03	0.97±0.03	1.0
1227	δ	−67.7 ± 2.9	12.9 ± 4.1	−8.5 ±1.4	−7.0 ±1.5	−10.7 ±1.0	−16.0 ±1.0	0.3 ±0.7	3.4 ±0.6	−0.1 ±0.7
	ρ	0.53± 0.03	0.25± 0.04	0.49±0.03	0.76±0.03	0.75±0.03	0.59±0.02	1.0	0.85±0.02	1.0
1300	δ	−52.8 ± 3.8	18.8 ± 4.1	−20.2 ±1.8	−7.4 ±1.4	−14.2 ±1.5	−13.9 ±1.7	4.5 ±1.0	2.4 ±0.7	1.9 ±0.9
	ρ	0.29± 0.05	0.27± 0.05	0.67±0.03	0.76±0.03	0.62±0.03	0.53±0.02	$0.99_{-0.02}^{+0.01}$	0.84±0.03	1.0
1446	δ	−82.0 ± 5.2	11.1 ± 5.9	−13.9 ±7.0	11.0 ±2.7	−5.4 ±5.7	−2.1 ±1.6	−3.3 ±7.1	3.0 ±1.3	−1.2 ±1.1
	ρ	0.29± 0.05	0.45± 0.06	0.76±0.05	0.78±0.06	0.31±0.06	0.98±0.02	0.60±0.03	1.0	0.81±0.02
1560	δ	24.0 ±10.0	4.6 ± 4.5	−18.8 ±7.0	−1.6 ±4.4	1.1 ±4.6	7.6 ±1.9	1.0 ±1.9	4.1 ±1.0	−3.2 ±1.5
	ρ	0.58± 0.14	0.84± 0.09	0.10±0.07	0.68±0.07	0.34±0.05	0.75±0.09	0.59±0.07	$0.99_{-0.04}^{+0.01}$	0.76±0.05

(b) The real and imaginary part of the partial amplitudes: $\mathrm{Re}a = \frac{1}{2}\rho \sin 2\delta$, $\mathrm{Im}a = \frac{1}{2} - \frac{1}{2}\rho \cos 2\delta$. (Those two combinations of the parameters are sometimes more useful than the phase and absorption themselves.)

(c) The real and imaginary part of the B amplitude associated with the spin-flip amplitude:

$$\frac{1}{4\pi\lambda^3}B = \sum_l \{l(l+E/m)a_l^- - (l+1)(l+1-E/m)a_l^+\}.$$

[Eq. (A16) in Appendix]

This combination of amplitudes is very sensitive to the higher partial waves. The real part of the forward scattering amplitude $f(0°)$,

$$\mathrm{Re}F(0°) = \lambda \sum_l [(l+1)\,\mathrm{Re}a_l^+ + l\,\mathrm{Re}a_l^-],$$

[Eq. (A15) in Appendix]

is also a sensitive combination of the partial-wave amplitudes, but, as the 0° cross section was fed in the program, the fitted value of $\mathrm{Re}F(0°)$ was always well inside the errors quoted for the calculated dispersion-relation value. So it does not bring any useful additional constraint for continuity.

(d) The coefficients D_n of the expansion of $(1/\lambda^2 \sin\theta) \times P(d\sigma/d\Omega)$ in Legendre polynomials. This is particularly useful for energies where no polarization or only inaccurate ones exist.

In practice, this was done by plotting the variation with energy of all the preceding parameters. For a given solution, as soon as one of those quantities could not be joined with the corresponding one at neighboring energies without a physically unacceptable discontinuity, that solution was discarded.

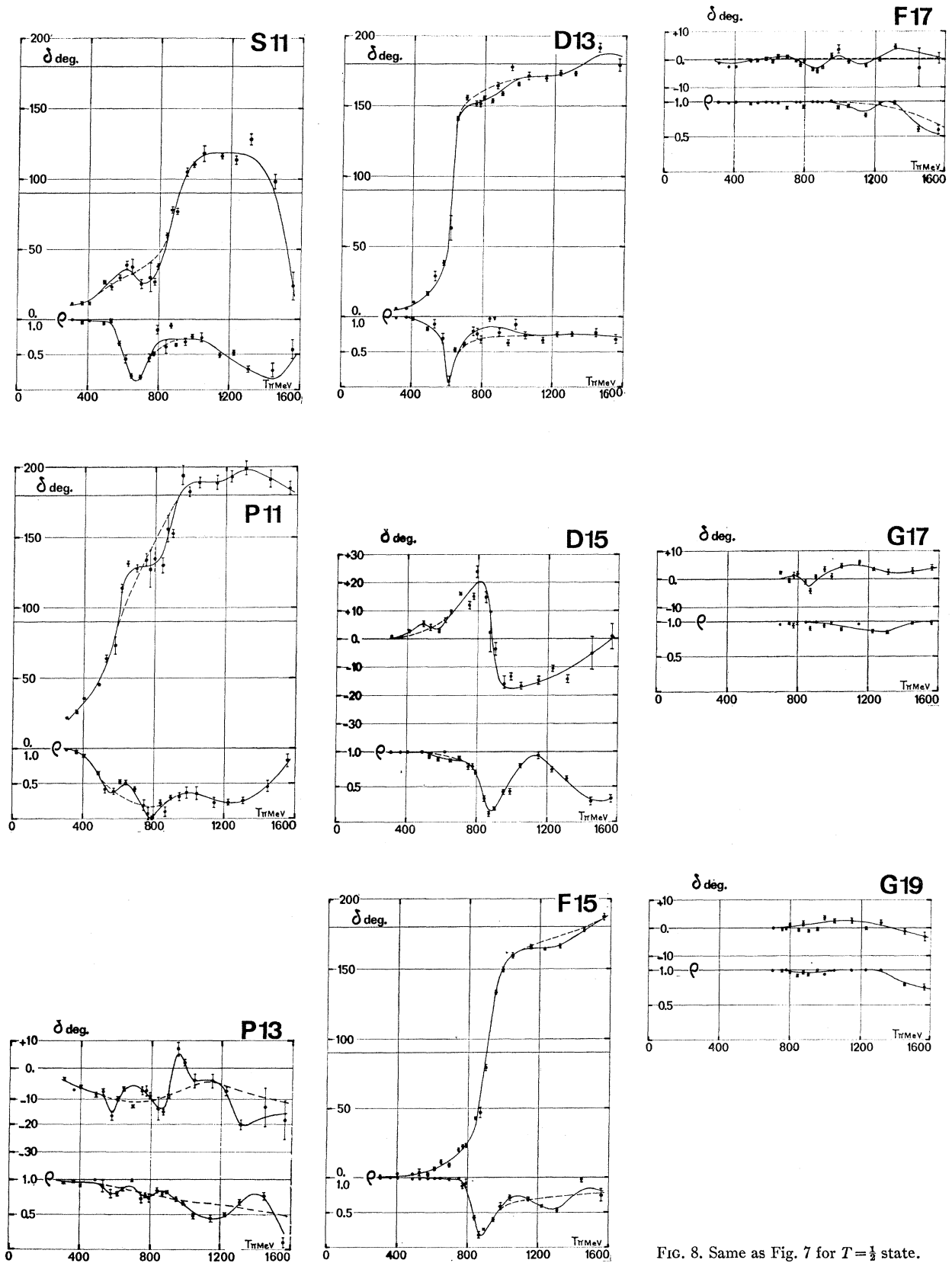After this second stage, the number of remaining

FIG. 8. Same as Fig. 7 for $T = \frac{1}{2}$ state.

TABLE III. Number of experimental data used for each energy.

T_π (MeV)	Number of experimental data						Total χ^2		χ^2/N		References
	σ^+	P^+	σ^-	P^-	σ^0	Total[a]	Sol. A	Sol. B	Sol. A	Sol. B	
310	24	4	29	30	13	104	108.6		1.25		27, 12, 13, 14, 15, 16, 17
	24	4	29	6	13	80	76.2		1.16		
370	18		24	6	12	64	45.8		1.04		18, 19, 15
410	35	12	36	12		99	90.9		1.16		18, 20, 21
492	40	12	33	12	20	121	98.7	137.8	0.99	1.38	18, 20, 21, 22, 23
533	16	8	16	9	21	74	39.8	56.3	0.8	1.13	24, 25, 26, 23
581	17	10	17	11	21	80	80	120.8	1.43	2.16	24, 25, 26, 23
618	21	10	11[b]	27	21	94	57.4	98	0.8	1.36	18, 11, 28
650	21		21		21	67	62.4	92.2	1.45	2.15	18, 23
698	18	9	18	26	21	96	72	129.3	1.1	2.0	24, 25, 26, 11, 23
750	19	4	19	16	21	83	61.2	106.4	1.2	2.1	29, 30, 28
775	11[b]	11	21	27	11[b]	85	47.8	113.5	0.89	2.1	11, 31
795	19		19	16	11[b]	69	48.4	235.6	1.31	6.4	29, 30
845	19	14	19	16	21	93	80.8	378.8	1.34	6.31	29, 30, 28
873	18	11	19	13	21	86	63.7	394	1.18	7.3	29, 30, 32, 23
900	19	14	19	16	21	93	79.8	322	1.33	5.54	29, 11, 30, 28
950	19	13	19	16	11[b]	82	48.56	202.4	0.95	3.97	29, 11, 30
990	20	14	20	14	21	93	54.9	202	0.93	3.43	24, 32, 26, 23
1048	19	17	19	24	11[b]	94	77.72	655.1	1.3	10.9	29, 11
1150	19	25	18	16	21	103	72.6	326.0	1.07	4.79	29, 11, 30, 28
1227	19	22	19	23	11[b]	98	73.3	442	1.13	6.8	29, 11, 30
1300	20	30	19	16	21	110	83.6	314	1.1	4.14	24, 11, 29, 30, 23
1446	18	24	19	16		81	44.7	215	0.95	4.57	29, 11, 30
1560	21	25	34	26	21	131	65.17		0.68		24, 11, 33, 34, 35

[a] The total number in column 7 includes also 4 points for the total and total inelastic cross sections. In columns 8 and 9 we give the resulting χ^2 for the solutions A and B, and in 10 and 11 the same χ^2 divided by the number of degrees of freedom.
[b] The corresponding points are calculated from interpolation on the coefficients of the expansion of the angular distributions.

solutions is greatly reduced, but, unfortunately, there are energies where there is more than one solution left. However, even when there are still 2 to 5 solutions left, most of the phase shifts are nicely grouped and almost identical within the errors. But the problem is not always satisfactorily solved, especially for the low angular momenta, where (i) S_{11} (between 0.6 and 0.85 GeV, and above 1.2 GeV), (ii) P_{11} (between 0.6 and 0.9 GeV), and (iii) P_{13} (between 0.5 and 1 GeV), present two slightly different behaviors. Also, above 1.3 GeV we were faced with some difficulties to get continuity.

To solve these two possibilities, we required that the unambiguous phase shifts, corresponding mainly to high angular momenta, have a smooth energy variation, whereas beforehand small discontinuities were accepted. These smoothed values were then used as input to the minimization program.

The two behaviors observed for low angular momenta (i, ii, iii) then merged together: the resulting solution is shown in Figs. 7 and 8.

We have tried to resolve the ambiguity arising above 1.3 GeV with the same method. In that region, the energies where the analysis is possible are more spaced and we are also close to the end of the range, so that the selection is less clear. We show the most probable solution, i.e., that with the best χ^2. The other possibility, however, is not very different, and this difference affects only the small waves.

It should be noted that when performing this last selection two solutions compatible within the errors have not been considered as different.

The errors given are statistical only. The meaning of the error on the value x of a parameter is that the best χ^2 obtained with the value $x+dx$ or $x-dx$ is greater by 1 than that found for x, all other parameters being able to move freely. We do not claim that it is the real relevant error from the point of view of physics but it is the only one which has a definite meaning, reflecting the form of the χ^2 hypersurface near the minimum. Given a certain solution, by fixing any one of the parameters at a much different value, it is sometimes possible to get a rather good χ^2, but then the other parameters are obliged to take values very different from the initial ones, showing that we are in presence of a different minimum not linked with the previous one. On Figs. 7 and 8 the final solution for all the energies where the analysis was done is given. The corresponding values are given in Tables I and II. The solution resulting from the smoothing done by hand on the real and imaginary parts of the partial-wave amplitudes, as explained above, is shown in curve A in Figs. 7 and 8. At some energies and waves, the points are rather far from the curve; this is so because a curve passing through all the points would lead to an unreasonably fast oscillating behavior. We have tried unsuccessfully to obtain more continuous solutions for those energies. In fact, we feel allowed to put more or less weight on certain energies. For instance: At 870 MeV the polarization data are old and not accurate (see Fig. 6). The $\pi^\pm p$ angular distributions have been measured in two different laboratories; in $\pi^+ p$ they are incompatible (see comparison in Ref. 42). Here there seem to be important systematic
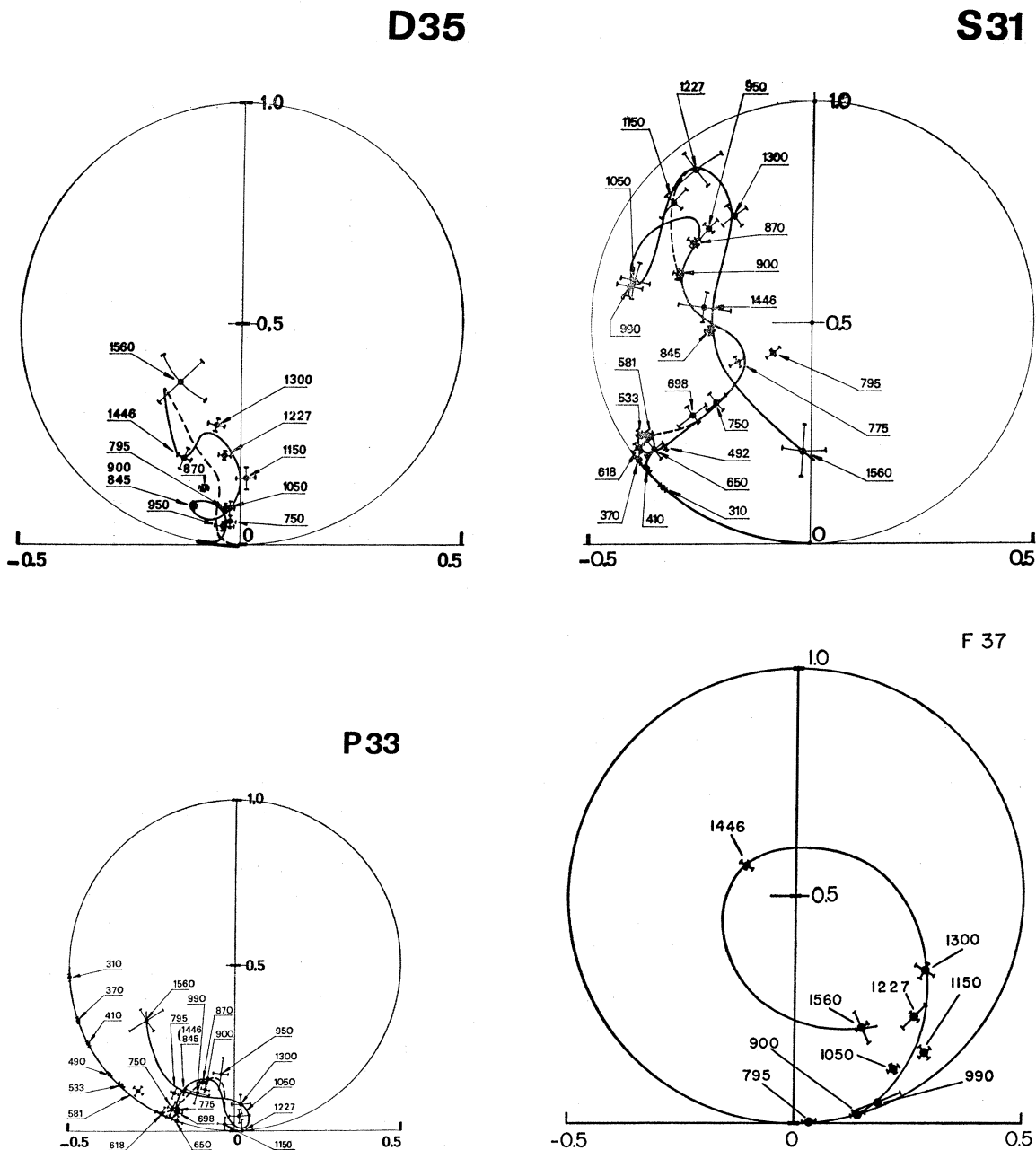
D35   **S31**

P33   F 37

FIG. 9. Plot of the amplitude of some waves in the complex plane for $T = \frac{3}{2}$ state.

errors. At 795 MeV, the $\pi^+ p$ polarization is missing and we were obliged to construct the charge-exchange angular distribution from the C_n^0 coefficients. At 950 MeV, the $(d\sigma/d\Omega)_{\pi^0 n}$ is also constructed.

An other smoothing has been done, which erases all the small irregularities (see solution B, Figs. 7 and 8). If we try to get solutions corresponding to the B smoothing allowing a maximum variation of 3° for the phases and 0.03 for the absorptions, the resulting total $\chi^2 = 4928$ is very high (to be compared to $\chi^2 = 1633$ for

solution A; see Table III). When the constraints on the parameters are released, they drift towards the values corresponding to solution A. This proves that those effects are required by the experimental data used. In an energy-dependent analysis, where a continuity is obtained by imposing a specific kind of variation for the amplitudes or phases, the final solutions could be at best like our solution B. The number of parameters needed to get a solution like A would be very large. Moreover, a random search seems to be excluded due to
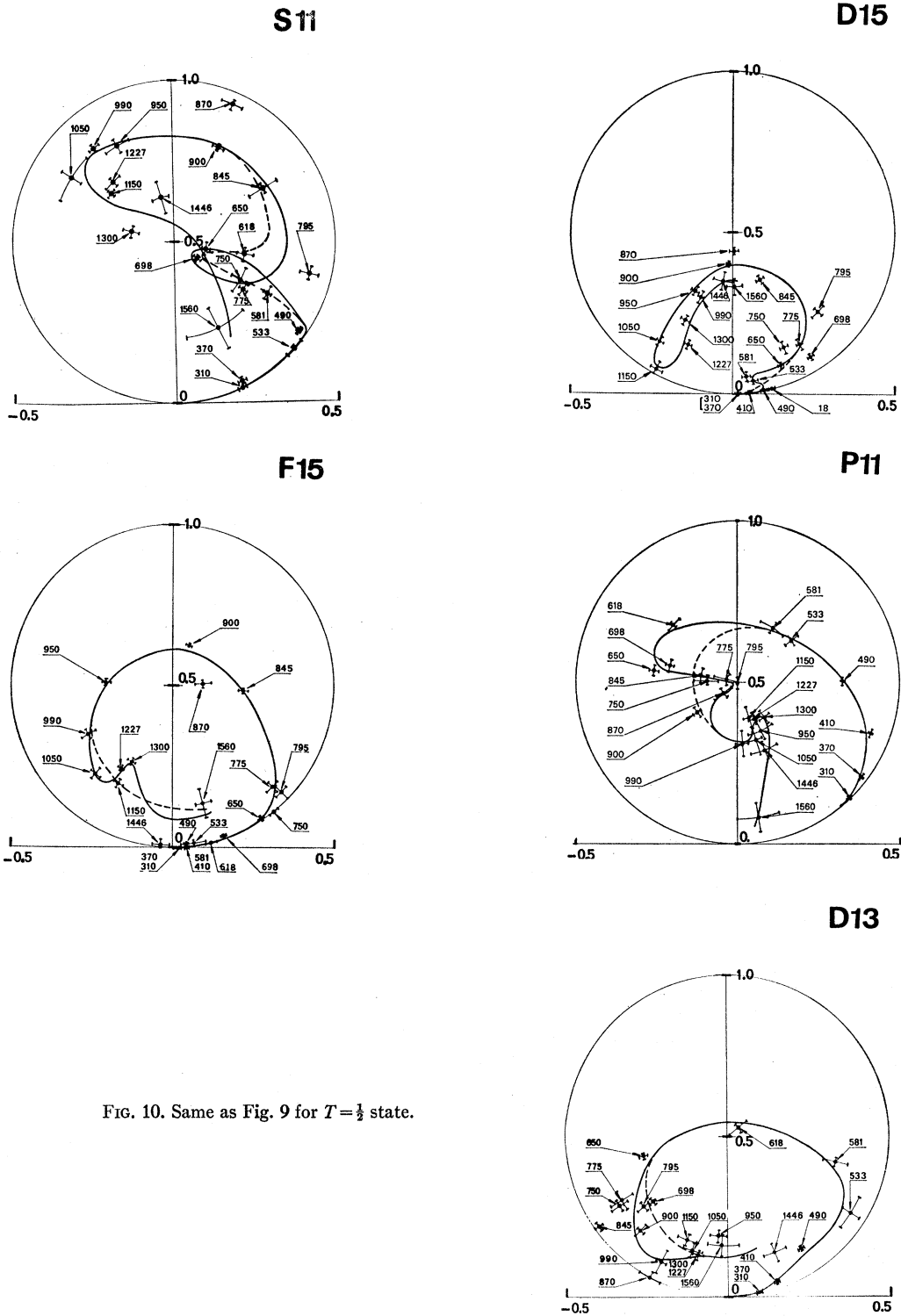
S11

D15

F15

P11

FIG. 10. Same as Fig. 9 for $T = \frac{1}{2}$ state.

D13

the large number of experimental data that must be fed in; the final solution reached will never be far from that used as input. In an energy-dependent fit it should be possible to detect if there are any isolated wrong

experimental data. In fact, in our solution B the very high X^2 obtained for most of the energies is not due to all data equally, some data contributing more than others. However, those measurements cannot be eliminated on

FIG. 11. Partial-wave cross sections computed from the solution A. σ_{tot}, solid curves; σ_{el}, dot-dashed curves; σ_{inel}, dashed curves; rate of variation of the amplitude, dotted curves. Vertical scale: 2 mb by step.

TABLE IV. Mass and width of the resonant states estimated from the partial cross section and from the rate of variation with energy of the amplitude, and approximate elasticity. The accuracy for mass and widths is not better than 20 MeV. Elasticities are taken at the maximum of σ_{tot} with an accuracy of about 0.1.

State $l_{2I,2J}$	From total cross section M (MeV)	Γ (MeV)	From velocity in complex plane M (MeV)	Γ (MeV)	Estimated elasticity $x = \Gamma_{el}/\Gamma_{tot}$
S_{31}	1695	250	1650	130	...
P_{33}^a	1240	110	...	...	1
F_{37}	1975	180	1980	140	0.57
S_{11}	1535	155	1515	105	...
S_{11}	1710	260	1665	110	
P_{11}	1470	255	1505	205	0.68
D_{13}	1510	125	1515	110	0.54
D_{15}	1680	135	1655	105	0.41
F_{15}	1690	110	1680	105	0.64

a These values come from Ref. 6.

the Thirteenth High Energy Conference of Berkeley, show the same big effects as the solution presented here. The irregularities are even sometimes larger than in our solution.

The predictions of Hamilton et al.[46] for the non-resonating waves under 600 MeV are in good agreement with our result; at higher energies a comparison with the theory would also be of interest.

IV. DISCUSSION

Many of the partial waves found in this analysis present a strong energy dependence, as shown by the plot of the corresponding amplitudes (Figs. 9 and 10). The main interest of such an analysis is the possibility of discovering new resonancelike phenomena.

It is well known that when a purely elastic wave resonates it describes the unitarity circle in a counter-clockwise direction. When there is also an open inelastic channel and if the ratio of inelastic to elastic channels is constant, the amplitude also describes a circle with the center on the imaginary axis and diameter less than 1. If the elasticity is not constant this circle can be strongly distorted. In a more general situation the resonant effect will be superposed to a background scattering. Due to this superposition and the resulting interference, the circular behavior of the amplitude could be completely destroyed.[47] When one is in the presence of an amplitude whose trajectory describes a portion of a circle in the right direction and with a fast rate of variation with energy, one is tempted to attribute this behavior to a resonance in that amplitude. However, it is difficult to attribute a mass and a width to those resonances. Without knowledge of the physical process involved we used two methods for the determination of the parameters: one is based on the partial-wave total cross section, the other on the rate of varia-

this basis only, because they are usually part of a series of measurements done at several energies by a single group of experimenters using the same method and apparatus.

As no dependence of the parameters with energy is supposed, it is not possible to quote on over-all probability of the fit covering all energies, as done in energy-dependent analyses.

Our method would be inadequate if important discontinuities (cusps or other mechanisms) are expected. However, we feel that an important discontinuity is quite improbable. In any case, a theoretical knowledge of it would then be necessary for any kind of analysis. For the energy-dependent fits, it is even more difficult to cope with discontinuities. A cusp in S_{11} at the η threshold has been found in the analysis of Ref. 5 only because it was forced in the parametrization; it was not observed in Ref. 3, where the parametrization did not include it a priori.

The solution of Lovelace is basically an energy-independent fit; however, partial-wave dispersion relations are used in addition to the experimental measurements. We refer to Ref. 45 for the description of this method. The solutions, which have been presented at

[45] A. Donnachie, 1966 Edinburgh Lecture Notes, CERN Report 66/1042/5-TH.690, 1966 (unpublished).

[46] A. Donnachie and J. Hamilton, Phys. Rev. **138**, B678 (1965).

[47] R. H. Dalitz, Ann. Rev. Nucl. Sci. **13**, 339 (1964).

tion with energy of the partial-wave amplitude. By analogy with the elastic Breit-Wigner amplitude, the mass is taken at the maximum in both cases and the width is the width at half-maximum. The values given in Table IV are taken from Fig. 11. The accuracy on the given values is not better than 20 MeV, for masses and widths, and 0.1 for elasticities.

The S_{31} effect near a mass of 1650 MeV can be interpreted as an inelastic resonance superposed to a strong repulsive background. This background scattering could explain the fact that the two methods of evaluation of mass and width give different results (Table IV).

This resonance has also been observed in Ref. 48, where the background scattering has been evaluated from partial-wave dispersion relations. The parameters obtained are almost the same as ours. Near a mass of 1820 MeV another structure is apparent but the amplitude describe a clockwise trajectory in the complex plane.

The established F_{37} resonance is found at a higher mass (1975 MeV) than the bump observed in $\pi^+ p$ total cross section. This resonance is of the quasi-elastic type (phase crossing 90°). This behavior as compared to the one obtained in Ref. 6 could be confirmed when more experimental data will be available.

Except for the resonances described above and the well known P_{33} resonance, the waves in the $I = \frac{3}{2}$ isospin state present some structures, mainly inelastic. For instance, the behavior of P_{33} and D_{35} in the complex plane is shown in Fig. 9.

A strong inelastic effect in the S_{11} state appears near a mass of 1535 MeV. It has been correlated to the rise above threshold of the η-production cross section. Various interpretations have been obtained (see for instance Ref. 49 and quoted references). A second effect mainly elastic arises at about 1700 MeV. The behavior of S_{11} below 1 GeV has been interpreted with a general formulation[50] as the sum of an inelastic and an elastic resonance. Using the behavior of the S_{11} amplitude in the complex plane found in our previous analysis,[2] this method gives, respectively, 1570 and 1700 MeV for the masses, and 130 and 240 MeV for the widths.[50]

We found the P_{11} resonance at about 1470 MeV with a large width. This mass differs from that obtained by isobars excitation in proton-proton scattering ($\simeq$1400 MeV).[51] If the 1400-MeV missing-mass bump is due to this resonance, the shift in mass could probably be explained by production mechanisms.

In addition, Table IV gives the parameters of the well-known resonances in the D_{13}, D_{15}, and F_{15} states.

The structures in the other waves for the $I = \frac{1}{2}$ isospin state appear quite peculiar in the complex plane. As for the $I = \frac{3}{2}$ state, these effects are mainly inelastic and some cusps or inelastic resonances could be present. However, due to the very small elasticities (smaller than 0.2) and the limited accuracy of the available data, no reliable information can be obtained from those structures. We expect that work on inelastic pion-nucleon scattering done currently at Saclay and Berkeley could clarify the situation.

V. CONCLUSION

The aim of an analysis of this type is to detect the important phenomena which take place in the pion-nucleon interaction. In fact, we think that no big effect has been missed.

The experiments do not yet permit the determination of the phase shifts with an uncertainty smaller than a few degrees.

It seems important to know whether the small structures of the partial amplitudes observed here have a real meaning or not. This would imply not only new measurements like the polarization of the neutron in charge-exchange or the rotation parameters, but also experiments of a totally new kind where both statistical and systematic errors would be reduced by one order of magnitude. Those new measurements would also be useful if, for theoretical reasons, smaller errors were as necessary at high energies as they are in the low-energy range (determination of scattering length,[52] final-state interaction in Λ^0 decay,[53] etc.).

ACKNOWLEDGMENTS

APPENDIX: DERIVATION OF FORMULAS

The S matrix for elastic π-N scattering can be written as[7]

$$S_{fi} = \delta_{fi} - i(2\pi)^4 \delta(p_1 + q_1 - p_2 - q_2)$$

$$\times \left(\frac{m^2}{4E_1 E_2 w_1 w_2} \right)^{1/2} \bar{u}_2 T_{fi} u_1, \quad (A1)$$

where q_1, q_2 and p_1, p_2 are the initial and final four-

[48] A. Donnachie, A. T. Lea, and C. Lovelace, Phys. Letters **19**, 146 (1965).
[49] A. T. Davies and R. G. Moorhouse, Nuovo Cimento (to be published).
[50] C. Michael, Phys. Letters **21**, 93 (1966).
[51] E. W. Anderson, E. J. Bleser, G. B. Collins, T. Fujii, J. Menes, F. Turkot, R. A. Carrigan, Jr., R. M. Edelstein, N. C. Hien, T. J. McMahon, and I. Nadelhaft, Phys. Rev. Letters **16**, 855 (1966). See also the references quoted therein.

[52] J. Hamilton, Phys. Letters **20**, 687 (1966). V. K. Samaranayake, and W. S. Woolcock, Phys. Rev. Letters, **15**, 936 (1965).
[53] O. E. Overseth, and R. F. Roth, Phys. Rev. Letters **19**, 391 (1967).
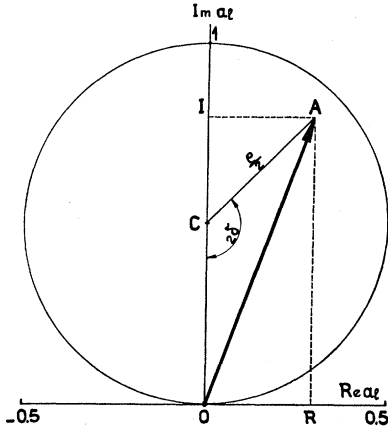
FIG. 12. Graphical method to represent ρ and δ in the complex plane.

momenta of the pions and of the nucleons,

$$E_i = (m^2 + \mathbf{p}_i{}^2)^{1/2}, \quad w_i = (\mu^2 + \mathbf{q}_i{}^2)^{1/2} \quad (i = 1, 2),$$

where m and μ are the nucleon and pion masses. u_1 and u_2 are the Dirac spinors for the initial and final nucleon states.

The invariant scattering amplitude T is of the form

$$T_{fi} = -A_{fi} + i\gamma \cdot Q B_{fi}, \tag{A2}$$

where $Q_\mu = \frac{1}{2}(q_1 + q_2)_\mu$ and γ_μ are the Dirac matrices. A and B are scalar invariant functions. Since phase shifts are used, it is useful to express the amplitudes A and B in terms of partial-wave π-N amplitudes.

The transition amplitude T_{fi} is related to the 2×2 Pauli scattering matrix M by

$$\langle f | M | i \rangle = -(m/4\pi W) \bar{u}_2 T u_1, \tag{A3}$$

where $|i\rangle$ and $|f\rangle$ are Pauli spinors for the initial and final nucleon spin states and W is the total energy in the c.m. system.

The requirement of parity conservation allows writing M in the form

$$M = f(\theta) + ig(\theta)\boldsymbol{\sigma} \cdot \mathbf{n}, \tag{A4}$$

where $\boldsymbol{\sigma}$ is the Pauli spin operator for spin $\frac{1}{2}$, $\mathbf{n} = \mathbf{q}_1 \times \mathbf{q}_2 / |\mathbf{q}_1 \times \mathbf{q}_2|$ and $\cos\theta = \mathbf{q}_1 \cdot \mathbf{q}_2 / |\mathbf{q}_1 \cdot \mathbf{q}_2|$, ($\mathbf{q}$ = pion momenta in the c.m. system).

f and g are the non-spin-flip and spin-flip amplitudes, respectively. Their expansion in terms of the scattering amplitudes $a_l{}^\pm$ is

$$f(\theta) = \lambda \sum_l \left[(l+1)a_l{}^+ + la_l{}^- \right] P_l(\cos\theta),$$
$$\tag{A5}$$
$$g(\theta) = \lambda \sum_l \left[a_l{}^- - a_l{}^+ \right] P_l{}'(\cos\theta),$$

where

$$a_l{}^\pm = (1/2i)\left[\rho_l{}^\pm e^{2i\delta_l{}^\pm} - 1 \right]. \tag{A6}$$

$\delta_l{}^\pm$ is the phase shift and $\rho_l{}^\pm$ the absorption parameter

for scattering in the states with $J = l \pm \frac{1}{2}$. $\lambda = \hbar/q$ is the Compton wave length of the pion.

In terms of isospin amplitudes the observable amplitudes are

$$a_l{}^{\pm+} = a^{(3/2)},$$
$$a_l{}^{\pm-} = \frac{1}{3}(a_l{}^{\pm\,(3/2)} + 2a_l{}^{\pm\,(1/2)}), \tag{A7}$$
$$a_l{}^{\pm0} = (\sqrt{2}/3)(a_l{}^{\pm\,(3/2)} - a_l{}^{\pm\,(1/2)}),$$

where the superscripts mean

$$+ \sim \pi^+ p \rightarrow \pi^+ p,$$
$$- \sim \pi^- p \rightarrow \pi^- p,$$
$$0 \sim \pi^- p \rightarrow \pi^0 n,$$

$\frac{3}{2}$ and $\frac{1}{2}$ are the two isospin states of the π-N system. The measurable quantities are given in terms of the partial amplitudes $a_l{}^\pm$ as follows.

Differential cross sections:

$$d\sigma/d\Omega = |f|^2 + |g|^2. \tag{A8}$$

The cross section can be expanded in Legendre polynomials:

$$d\sigma/d\Omega = \lambda^2 \sum_{n=0}^{2l\text{max}} C_n P_n(\cos\theta), \tag{A9}$$

with

$$C_n = \sum_{ll'JJ'} \alpha_n \, \text{Re}(a_{lJ}{}^* a_{l'J'}). \tag{A10}$$

Recoil nucleon polarization:

$$\mathbf{P}(\theta) = \frac{2\,\text{Im} f^* g}{|f|^2 + |g|^2} \cdot \mathbf{n}. \tag{A11}$$

The expression

$$\frac{1}{\sin\theta} P \frac{d\sigma}{d\Omega} = \lambda^2 \sum_{n=0}^{2l\text{max}-1} D_n P_n(\cos\theta) \tag{A12}$$

is expanded in Legendre polynomials and gives

$$D_n = \sum_{ll'JJ'} \beta_n \, \text{Im}(a_{lJ}{}^* a_{l'J'}). \tag{A13}$$

Forward scattering: The forward elastic cross section is given by

$$\sigma(0°) = [\text{Re} f(0°)]^2 + [\sigma_{\text{tot}}/4\pi\lambda]^2, \tag{A14}$$

where the second bracket comes from the optical theorem.

$$\text{Re} f(0°) = \lambda \sum_l \left[(l+1) \, \text{Re} a_l{}^+ + l \, \text{Re} a_l{}^- \right]. \tag{A15}$$

The B amplitude can be expressed in terms of partial amplitudes:

$$\frac{1}{4\pi} B = \frac{\lambda}{E+m} \sum_l \left[a_l{}^+ P_{l+1}{}'(\cos\theta) - a_l{}^- P_{l-1}{}'(\cos\theta) \right]$$
$$+ \frac{\lambda}{E-m} \sum_l (a_l{}^- - a_l{}^+) P_l{}'(\cos\theta).$$

This expression can be put in the form

$$\frac{1}{4\pi\lambda^3}B=\sum_l\{l(l+E/m)a_{l^-}-(l+1)(l+1-E/m)a_{l^+}\}.\tag{A16}$$

Representation of $a_{l^\pm}$ in the complex plane (Argand diagrams): Figure 12 gives a simple method to construct a_l in terms of δ and ρ. Conservation of probability imposes that a_l be inside the "unitary circle" centered at the point $(0,i/2)$ and with radius $\frac{1}{2}$.

Partial cross sections are given by

$$\sigma_{\text{tot}}=\sigma_{\max}(1-\rho\cos2\delta)/2=\sigma_{\max}(OI),$$

$$\sigma_{\text{el}}=\sigma_{\max}(1+\rho^2-2\rho\cos2\delta)/4=\sigma_{\max}(OA)^2,$$

$$\sigma_{\text{inel}}=\sigma_{\max}(1-\rho^2)/4=\sigma_{\max}[1-4(CA)^2]/4,$$

with

$$\sigma_{\max}=4\pi\lambda^2(J+\tfrac{1}{2}).$$

Calculation of the Low-Energy S-Wave Pion-Pion Interaction from the K_{e4} Decay Using Charge Commutation Relations*

S. Matsuda and S. Oneda

Department of Physics and Astronomy, University of Maryland, College Park, Maryland

(Received 2 August 1967)

By making use of an appropriate charge commutation relation, we have computed the low-energy pion-pion scattering length directly from the rate of K_{e4}-decay. The main differences from previous approaches are as follows: (a) Instead of using the current commutation relations (which have been extensively used with the soft-pion technique), we stick to the better-known charge commutation relations. This enables us, as in the Adler–Weisberger calculation, to avoid taking the usual soft-pion limit $k_\mu\to0$; instead we let only $k^2(=-m_\pi^2)\to0$, which is certainly a smaller extrapolation. (b) In contrast with previous calculations of K_{e4} decays, which utilized essentially the kaonic PCAC $(m_K\to0)$, we use the pionic PCAC, which involves a much smaller extrapolation $(m_\pi\to0)$. From the presently available K_{e4} decay rate, we have estimated the values of the $I=0$ and 2 S-wave pion-pion scattering length as $a_0\simeq0.18$ and $a_2\simeq-0.017$. Although our numerical results for a_0, a_2, and the K_{e4}-decay form factors turn out to be not very different from those obtained by using the current commutation relations with soft-pion techniques, we emphasize the important difference between the two approaches mentioned in (a) with respect to the extrapolation procedures.

THE K_{e4} decay has been known to be one of the best places to study the low-energy pion-pion interaction. At the moment, experiments do not allow a definite conclusion. They give for the $I=0$ S-wave pion-pion scattering length the value[1]

$$a_0=(0.6_{-0.5}^{+0.6})m_\pi^{-1}.\tag{1}$$

Theoretically, the strength of the low-energy pion-pion interaction is of crucial importance for judging the physical significance of a large number of calculations employing current algebra. The apparent success of the soft-pion emission technique based on the current commutation relations (CCR), which, for instance, relates the $K\to3\pi$ amplitude to the $K_1^0\to2\pi$ amplitude[2] and also the leptonic decay amplitudes of the

K meson,[3,4] is hard to understand unless the value of a_0 is small. In fact, by using CCR and the hypothesis of partially conserved axial-vector current (PCAC) and by *assuming that the scattering length in question is small*, Weinberg,[5,6] for instance, did indeed obtain a small $I=0$ S-Wave π-π scattering length:

$$a_0=0.20m_\pi^{-1}.\tag{2}$$

However, the procedure used in deriving the value given by Eq. (2) is not entirely free from theoretical ambiguity, especially with respect to the off-mass-shell extrapolation procedure. It has been pointed out that one could obtain a family of solutions which contains

[1] This value is presented by R. W. Birge *et al.*, in *Proceedings of the Thirteenth International Conference on High-Energy Physics, Berkeley, California, 1966* (University of California Press, Berkeley, Calif., 1967), p. 37; see also, R. W. Birge, R. P. Ely, G. Gidal, G. E. Kalmus, A. Kernan, W. M. Powell, U. Camerini, D. Cline, W. F. Fry, J. G. Gaido, D. Murphree, and C. J. Murphy, Phys. Rev. **139**, B1600 (1965).

[2] M. Suzuki, Phys. Rev. **144**, 1154 (1966); C. G. Callan and S. B. Treiman, Phys. Rev. Letters **16**, 153 (1966); Y. Hara and Y. Nambu, *ibid.* **16**, 875 (1966); L. J. Clavelli, Phys. Rev. **160**,

1384 (1967); D. K. Elias and J. C. Taylor, Nuovo Cimento **44A** 518 (1966); H. D. Abarbarnel, Phys. Rev. **153**, 1547 (1967).

[3] C. G. Callan and S. B. Treiman (Ref. 2); M. Suzuki, Phys. Rev. Letters **16**, 212 (1966); V. S. Mathur, S. Okubo, and L. K. Pandit, *ibid.* **16**, 371 (1966); L. J. Clavelli, Phys. Rev. **154**, 1509 (1967).

[4] S. Weinberg, Phys. Rev. Letters **17**, 336 (1966); **18**, 1178(E) (1967).

[5] S. Weinberg, Phys. Rev. Letters **17**, 616 (1966); see also, Y. Tomozawa, Nuovo Cimento **46A**, 707 (1966); A. P. Balachandran, M. Gundzik, and F. Nicodemi, *ibid.* **44A**, 1257 (1966); N. Khuri, Phys. Rev. **153**, 1477 (1967).

[6] F. T. Meiere, Phys. Rev. **159**, 1462 (1967); F. T. Meiere and M. Sugawara, *ibid.* **153**, 1702, (1967); **153**, 1709 (1967).